# Efficient Coherent Adaptive Representations of Monitored Electric Signals in Power Systems Using Damped Sinusoids

Lisandro Lovisolo, Eduardo A. B. da Silva, *Member, IEEE*, Marco A. M. Rodrigues, *Member, IEEE*, and Paulo S. R. Diniz, *Fellow, IEEE*

***Abstract*—This paper presents coherent representations of electric power systems signals. These representations are obtained by employing adaptive signal decompositions. They provide a tool to identify structures composing a signal and constitute an approach to represent a signal from its identified components. We use the Matching Pursuits algorithm, which is a greedy adaptive decomposition, that has the potential of decomposing a signal into coherent components. The dictionary employed is composed of damped sinusoids in order to obtain signal components closely related to power systems phenomena. In addition, we present an effective method to suppress the pre-echo and post-echo artifacts that often appear when using the Matching Pursuits. However, the use of a dictionary of damped sinusoids alone does not ensure that the decomposition will be meaningful in physical terms. To overcome this constraint, we develop a technique leading to efficient coherent damped-sinusoidal decompositions that are closely related to the physical phenomena being observed. The effectiveness of the proposed method for compression of synthetic and natural signals is tested, obtaining high compression ratios along with high signal-to-noise ratio.**

***Index Terms*—Coherent representations, damped sinusoids, matching pursuits, power systems transient analysis, signal compression, signal modeling, signal representations.**

## I. Introduction

DISTURBANCE monitoring is increasingly being required in contemporary top-quality power plants. The approach most relevant to this work is the post-event analysis of monitored signals. This analysis allows for the identification of patterns and characteristics of faults [1] in order to improve the knowledge of the system behavior and prevent future problems. The information is measured by digitizing the signals corresponding to the voltage and/or current quantities with a *Digital Fault Recorder* and storing them for future transmission and analysis in order to identify the different natural phenomena represented in the signal that took place in the course of the disturbance. In a broad sense, these techniques are called oscillography and can be divided into *Short-Time or Transient Oscillography*, in which sampled versions of the voltage and/or the current waveforms at points of the network are used for monitoring transient phenomena, protection systems, and equipment malfunctions, as well as for locating faults in time and space and also for power quality assessment. In *Long-Time Oscillography*, the power flow and the oscillations of the fundamental frequency are monitored and searched for low-frequency oscillations and slow transients; these provide information about the dynamic behavior of the interconnected network.

Regardless of the quantities measured, the net result of oscillography is the study of the evolution in time of various phenomena. In general, these phenomena are represented as sinusoidal oscillations of increasing or decreasing amplitudes. They are also highly influenced by circuit switching, as well as nonlinear power systems components and loads. The number of points monitored by oscillographic systems increases rapidly because system operation bounds are more critical as demand increases. In addition, at interconnected systems, it is necessary to establish precisely the causes of the disturbances as well as the parts responsible for the resulting effects.

The storage and transmission of oscillographic signals may generate an information overload; even though storage cost is decreasing, the general tendency is to sample signals at higher rates and using longer windows. Thus, storage capacity and transmission bandwidth problems persist, demanding good compression schemes. In order to obtain high compression ratios, lossy compression must be used. However, the compression must be such that the loss of quality involved does not impair the signal analysis. In addition, the information overload is a serious problem to disturbance analysis since human experts performing such analyses are not, in general, able to look through all available data. This creates a demand for computational tools that both enable efficient transmission and storage of the information and aid in the analysis of the phenomena. Therefore, a technique that decomposes a signal into components that are coherent to power system phenomena modeling would be welcome in automated analysis (for example, using expert systems techniques [1]).

This work proposes a procedure aimed at efficient representations of power systems signals for short-time oscillography such that their analysis is not impaired. The approach is to use a damped sinusoid signal model that is related to the phenomena typically observed at power system plants. The different components of a signal, each one associated with a different phe-

Manuscript received December 5, 2003; revised November 28, 2004. The associate editor coordinating the review of this manuscript and approving it for publication was Prof. Sheila S. Hemami.

L. Lovisolo is with the Universidade Federal do Rio de Janeiro, Rio de Janeiro, RJ, 21945-970, Brazil, and also with the Universidade do Estado do Rio de Janeiro, Rio de Janeiro, RJ, 20550-900, Brazil (e-mail: lisandro@lps.ufrj.br).

E. A. B. da Silva and P. S. R. Diniz are with the Universidade Federal do Rio de Janeiro, Rio de Janeiro, RJ, 21945-970, Brazil (e-mail: eduardo@lps.ufrj.br; diniz@lps.ufrj.br).

M. A. M. Rodrigues is with the Electric Energy Research Center, Rio de Janeiro, RJ, 21944-970, Brazil (e-mail: mamr@cepel.br).

Digital Object Identifier 10.1109/TSP.2005.855400

nomena, are identified through an algorithm based on Matching Pursuits [2], leading to an efficient representation of all relevant information. Thus, no important phenomenon is lost or distorted by the compression process; thus, a high compression ratio can be achieved while maintaining high signal-to-noise ratio (SNR).

After this brief introduction, Section II discusses some aspects of signal representations, including a review of the Matching Pursuits (MP) algorithm, which is the basis of the proposed method. In Section III, a model for power systems signals is proposed. Section IV reviews the Matching Pursuits with the Gabor Dictionary and proposes some improvements to it. In Section V, it is shown how to obtain decompositions according to the proposed model, along with heuristics that prevent MP deviation from a physically meaningful decomposition. Section VI describes how to obtain an automatic coherent representation with MP. The proposed algorithm is evaluated in Section VII by employing it to decompose and compress natural signals. Other applications of the method, such as denoising by synthesis and filtering, are presented in Sections VI-C and V-E. Conclusions are presented in Section VIII.

## II. Signal Representations

In general, any signal $\mathbf{x} \in \mathbb{X}$ can be represented by a linear combination (finite or infinite) of signals $\mathbf{g}_k$, provided that the set of signals $\mathbf{g}_k$, forming the dictionary $\mathcal{D}$, spans the space $\mathbb{X}$, or, in other words, is complete [2]. A signal $\mathbf{x}$ can be represented as a sum of predefined signals $\mathbf{g}_k$, $k \in \{0, 1, \ldots, K\}$ (in general, $\|\mathbf{g}_k\| = 1$) as [3], [4]

$$\mathbf{x} = \sum_{n=0}^{M-1} \alpha_n \mathbf{g}_{k(n)}. \tag{1}$$

Equation (1) decomposes the signal $\mathbf{x}$ as a linear combination of $M$ signals. Note that the dictionary may contain more elements than necessary to span the space $\mathbb{X}$, that is, $M$ may be larger than the dimension $N$ of the signal space. The key issue is how to obtain the coefficients $\alpha_n$ and the atoms $\mathbf{g}_{k(n)}$. Usually, a signal approximation is generated by using a number of atoms smaller than $M$. In general, this approximation improves as the number of atoms used increases. Usually, the dictionary must contain a very large number of structures $\mathbf{g}_k$ to enable the decomposition of (1) to coherently identify the different phenomena composing a signal. Indeed, the dictionary should contain distinct structures for any phenomena that we would potentially identify or discriminate, meaning that the dictionary may be quite large. That is why $K$ is, in general, larger than the dimension $N$ of the signal space. In this case, the dictionary is called redundant or overcomplete [3].

Power system disturbance signals provide a good illustration. These signals are composed of several concatenated or superimposed components (fundamental frequency, harmonics, transients, etc.). If a dictionary containing every possible phenomena represented in power system signals was built, then a redundant decomposition such as in (1) would have the potential of identifying each of these components. Although it is obviously impossible to construct such a dictionary, an alternative is to design a coherent dictionary (see 1 and 2 below, as well as Section VI).

In addition to redundancy, another desirable feature of signal representations is compactness [5], i.e., most of the signal energy should be concentrated in a small number of coefficients $\alpha_k$, corresponding to a small number of phenomena. One naturally asks the following: How do we combine both concepts, that is, to allow the identification of the structures in the signal employing a redundant representation while obtaining a compact representation of the signal? A good answer is given by adaptive representations [2]–[6].

Adaptive representations combine the points above by choosing, from a large dictionary, which atoms to use to represent a signal. This choice is signal dependent, hence, the term adaptive. These representations have been used in a wide range of applications: coding and compression, signal enhancement and denoising, pattern recognition, and understanding of signals [7]–[10].

There are still three aspects of signal representations that should be considered, especially in adaptive cases [3], [11]:

1) Are the functions being used to represent the signal coherent? That is, are they related to the possible phenomena composing the signal? A coherent dictionary would be one in which the atoms $\mathbf{g}_k$ are good models for the phenomena inherent to a given signal. This paper proposes in Section V the use of a dictionary of damped sinusoids for the representation of electric signals.
2) Are atoms being used in the decomposition to represent noise? Coherent representations are the ones in which the only significant atoms in the decomposition are those related to useful phenomena and not to noise. A key question is how to define which atoms correspond to coherent components and which ones correspond to noise. If such atoms can be identified, then we have a criterion to stop the decomposition. We will further explore this idea in Section VI-A.
3) Is the representation consistent [3]? This aspect concerns the similarity between the original signal $\mathbf{x}$ representation and its quantized version $\hat{\mathbf{x}}$. In [3], a consistent reconstruction is defined as follows: Given a signal $\mathbf{x} \in \mathbb{X}$ and a function $f : \mathbb{X} \to \mathbb{Y}$, $\mathbf{y} = f(\mathbf{x})$, if $f(\hat{\mathbf{x}}) = \mathbf{y}$, then $\hat{\mathbf{x}}$ is a consistent estimate of $\mathbf{x}$. Thus, consistency is related to how precisely the parameters representing the phenomena should be measured and/or quantized. Supposing the function $f$ is an expert analyst (human or system), a consistent reconstruction is obtained if the characteristics observed by an expert in the original signal and in its quantized representation are the same. Consistency of the proposed decomposition, in the above sense, is addressed in Sections V-E and VII through real-world (natural) examples.

To obtain a representation as the one in (1), based on some optimality criterion, is an NP-hard problem [6], that is, its complexity is not bounded by a polynomial of degree $N$ (the signal length). Some approaches lie on the selection of bases on which the signals are projected and represented [11], [12]. The optimum representation in these cases is the one that maximizes or minimizes a given criterion, considering that $M$ atoms are used to represent the signal. As an alternative, a suboptimal algorithm is used, namely the Matching Pursuits (MP), that has a large, but manageable, computational complexity.

### A. Matching Pursuits

The MP introduced by Mallat and Zhang [2] is a greedy adaptive approximation algorithm [6], [13]. At each step, the MP chooses the atom in the dictionary that best represents the signal (the atom with largest inner product with the signal). The chosen atom is then scaled and subtracted from the signal, and the process is repeated, representing the signal by progressive approximations.

Define a dictionary $\mathcal{D} = \{\mathbf{g}_\gamma\}$, $\gamma \in \Gamma$, ($\gamma$ is a set of parameters that define $\mathbf{g}$, and $\Gamma$ is the set of all possible $\gamma$), such that $\|\mathbf{g}_\gamma\| = 1$. If $\mathcal{D}$ is complete [2], [4], we can represent $\mathbf{x}$ as a sum of elements, that we call atoms or structures, of the dictionary $\mathbf{g}_{\gamma(n)}\,\mathbf{x} = \sum_n \alpha_n \mathbf{g}_{\gamma(n)}$. In order to compute the coefficients $\alpha_n$ and the indexes $\gamma(n)$, choose $\mathbf{g}_{\gamma(1)}$ such that $|\langle \mathbf{x}, \mathbf{g}_\gamma \rangle|$ is maximum, let $\alpha_1 = \langle \mathbf{x}, \mathbf{g}_{\gamma(1)} \rangle$, and then split $\mathbf{x}$ in two parts, defining the residue $\mathbf{R}^1_{\mathbf{x}} = \mathbf{x} - \alpha_1 \mathbf{g}_{\gamma(1)}$. Carrying out this process iteratively, we can compute the $(n+1)$th-order residue $\mathbf{R}^{n+1}_{\mathbf{x}}$ as

$$\mathbf{R}^{n+1}_{\mathbf{x}} = \mathbf{R}^{n}_{\mathbf{x}} - \alpha_{n+1} \mathbf{g}_{\gamma(n+1)} \tag{2}$$

where

$$\alpha_{n+1} = \left\langle \mathbf{R}^n_{\mathbf{x}}, \mathbf{g}_{\gamma(n+1)} \right\rangle \text{ and } \gamma = \arg \left\{ \max_{\gamma \in \Gamma} |\langle \mathbf{R}^n_{\mathbf{x}}, \mathbf{g}_\gamma \rangle| \right\}.$$

Properties of this algorithm as well as variations of it have been extensively studied [4], [10]. One of the most important properties of the MP is that the energy of the residue decreases monotonically at each approximation step, ensuring its convergence.

At each step of the MP, two pieces of information must be stored—the coefficient $\alpha_n$ and the index $\gamma_{(n)}$ defining the atom—and more information about the signal is extracted. Thus, at step $n$, we have an approximation of the signal based on the dictionary structures selected up to this step [4]; this means that the process can be halted, given a desired error criterion or a fixed number of steps. The obtained representation is adaptive since, at each step, the most similar structure to the signal is chosen from the dictionary $\mathcal{D}$ to decompose the signal. A compact representation can be obtained, provided that the number of atoms used in the decomposition is small. Therefore, the MP is capable of obtaining compact and efficient representations; the key to this lies in the choice of the dictionary $\mathcal{D}$, which should be coherent to the signal components. However, due to the greedy nature of MP, pre- and post-echo artifacts may appear (see Section IV-B), along with inefficiencies with respect to phenomena identification (see Sections V-B and D).

Summarizing, the MP decomposes a signal into a sequence of inner products $\alpha_n = \left\langle \mathbf{R}^{n-1}_{\mathbf{x}}, \mathbf{g}_{\gamma(n)} \right\rangle$ and indexes $\gamma(n)$. Fast algorithms exist for a limited number of $\gamma(n)$. However, for infinite possibilities of $\gamma(n)$, as employed here, there is no fast implementation. In this work, a method is proposed to reduce the complexity of the search for $\gamma(n)$ in the case of damped sinusoid structures.

## III. Building a Dictionary for Power Systems Signals

In order to analyze and compress signals from power systems, it is important to use a model capable of precisely representing the components that may compose those signals. Xu [14] defines the signal components in power systems as *Harmonics* are low-frequency phenomena ranging from 60/50 Hz (system fundamental frequency) to 3000 Hz. *Transients* are observed as impulses or high-frequency oscillations superimposed on the voltages or currents of fundamental frequency (60/50 Hz), as well as exponential (DC and modulated) components. *Sags* and *Swells* are increments or decrements, respectively, in the RMS voltage of duration from half cycle to 1 min (approximately).

In a very simplistic way, power systems can be considered to be built from transmission lines, sources, and loads. Transmission lines can be modeled by a series of distributed inductances, capacitances, and resistances. In these circuits, currents or voltages closely follow the solutions of differential equations. We should add to this model the discontinuities due to circuit switching caused by operative maneuvers and by the protection system. The proposal here is to generate a model for power system signals based on the solutions of linear differential equations that also incorporates these discontinuities. These solutions are given by an appropriate set of concatenated and superimposed damped sinusoids, each with a well-defined region of support. Therefore, the employed model is given by [15], [16]

$$f(t) = \sum_{q=0}^{Q-1} A_q \cos(2\pi f_q t + \phi_q) e^{-\rho_q (t - t_{s_q})} \times [u(t - t_{s_q}) - u(t - t_{e_q})] \tag{3}$$

where each component is a damped sinusoid represented by a six-tuple $(A_q, f_q, \rho_q, \phi_q, t_{s_q}, t_{e_q})$, where $A_q$ is its amplitude, $f_q$ is the frequency, $\rho_q$ is the damping factor, $\phi_q$ is the phase, and $t_{s_q}$ and $t_{e_q}$ are the component starting and ending times.

In this work, the analysis of power system signals will be restricted to frequencies that are integer multiples of a fundamental frequency $F$ ($f_q = K_q F$). Such harmonic analysis is appropriate for pseudo-periodic signals such as the power systems signals in question. It also simplifies the model and the best damped sinusoids matching search. Now, the six-tuple is given by $(A_q, k_q, \rho_q, \phi_q, t_{s_q}, t_{e_q})$, where $k_q = f_q/F$ is an integer. This model can effectively describe the relevant phenomena in electric power systems signals that are worth analyzing; therefore, being able to decompose a signal compactly and accurately in terms of these six-tuples and the model of (3) would be a powerful tool for analysis. The aim now is to develop an effective way to obtain this representation.

Note that the model in (3) by no means compactly represents "all" possible phenomena in power systems signals, as, for example, inrush currents or interharmonic oscillations (for $f_q = k_q F$). However, since the proposed dictionary is complete, then any signal can be represented as a linear combination of the atoms, although this representation may not be compact.

A similar model is obtained with the well-known Prony method [17]–[19] used in the analysis of power system signals (as well as in numerous other applications). It obtains a representation of the signal as $f(t) = \sum_{q=0}^{Q-1} A_q \cos(2\pi f_q t + \phi_q) e^{-\rho_q t}$. A drawback of the Prony method, for the desired application, is that it does not take into account the discontinuities due to circuit switching, i.e., it does not allow the damped sinusoids to start at different instants. Therefore, the proposed model can be seen as the Prony model with time localization capabilities. Another advantage is that the proposed method, when applied to obtain the

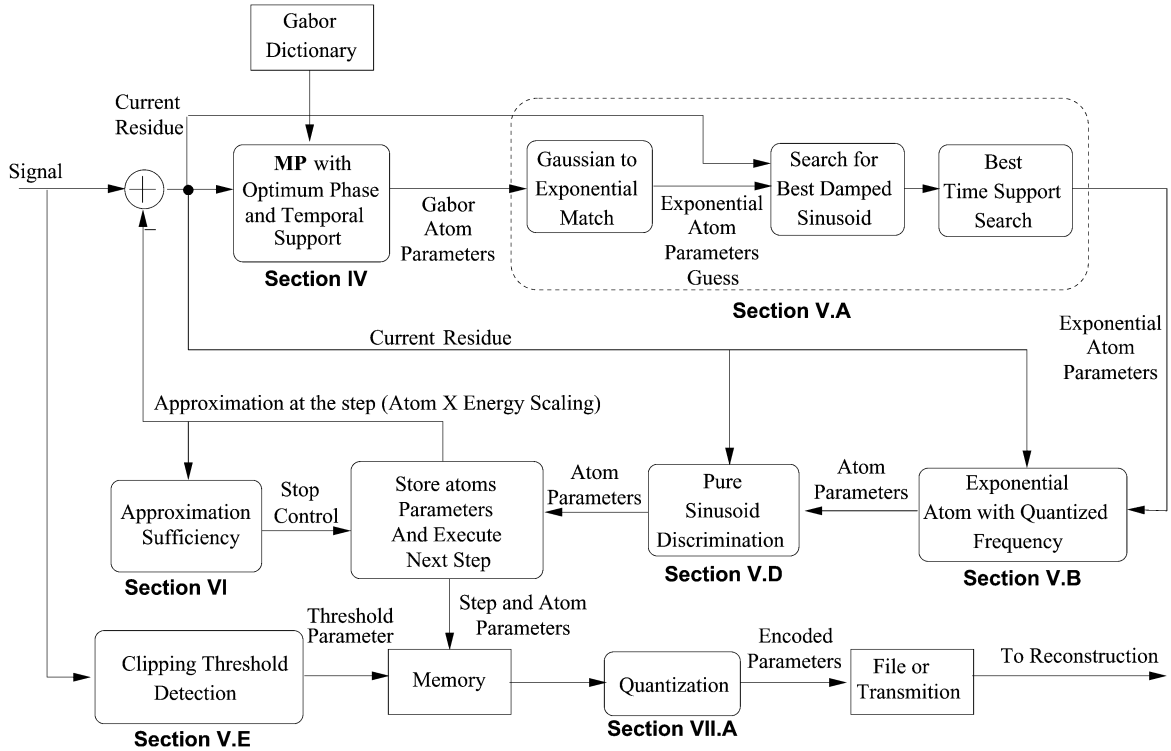


Fig. 1. Block diagram of the decomposition algorithm.

model, avoids the numerical instabilities inherent to the Prony method that might appear due to the matrix inversions required to compute the damping factors.

Using a dictionary of unit norm vectors, the structures of (3) are uniquely determined by the five-tuples ($k_qF$, $\rho_q$, $\phi_q$, $t_s$, $t_e$). Observe that this dictionary has a basis of impulses in time [five-tuples (0, 0, 0, $t$, $t$)], as well as a basis of impulses in frequency [five-tuples ($k_qF$, 0, 0, $-\infty$, $\infty$)] and is thus complete. However, in order to implement the MP algorithm, the parameters of the five-tuple ($k_qF$, $\rho_q$, $\phi_q$, $t_s$, $t_e$) must be discretized. Preliminary tests were held in this direction [16], but the results were not encouraging. One dictionary for which discretization processes are well known and have been extensively used is the Gabor dictionary [2], [4], [20]. The Gabor dictionary is composed of Gaussian functions modulated by sinusoids. Then, at each step, we decided to adopt the strategy of decomposing the signal using the MP with the Gabor dictionary as an intermediate solution and, then, from the parameters of the chosen Gabor atom, searching for the damped sinusoid that best matches the signal at that step. This approach gives an MP-based decomposition with good performance and feasible computational complexity. It is important to note that it is not claimed here that a solution using a direct discretization of the damped sinusoid dictionary is not feasible. Based on some preliminary results, we have simply chosen the strategy of first using the MP with the Gabor dictionary and then performing a search for the best sinusoid. Justifications for this strategy, in terms of computational complexity, are given in Section V-C.

A block diagram of the algorithm is shown in Fig. 1 (where the sections of this paper in which each topic is developed are also indicated). The process breaks the problem of finding the parameters in a five-dimensional space ($k_qF$, $\rho_q$, $\phi_q$, $t_s$, $t_e$) into several smaller-dimensional problems, each demanding less computational effort, thereby reducing the overall complexity. The first step is the decomposition of the current residue into a dictionary of Gabor atoms. The result of the decomposition at each step is used to match the current residue to a damped sinusoid instead of the Gabor atom. Then, for the damped sinusoid a frequency quantization is applied, as is a heuristic to select between damped or pure sinusoids. Then, the parameters of the resulting damped sinusoid structure are stored. The approximation sufficiency procedure is implemented to estimate whether the approximation already obtained is good enough or if the decomposition must continue. The parameters are quantized and encoded at the end of the decomposition process using different quantizers for each parameter.

## IV. Matching Pursuits With the Gabor Dictionary—Discussion and Improvements

The Gabor dictionary is generated by time shifting, scaling, and modulation of a Gaussian window $g(t) = 2^{(1/4)}e^{-\pi t^2}$ [4]. A Gabor atom is given by $g_\gamma(t) = (K_\gamma/\sqrt{s})g\left(t-\tau/s\right)\cos\left(\xi t+\phi\right)$, where $\gamma = (s,\tau,\xi,\phi)$ and is a well-localized time-frequency component [2]. For this $g(t)$, the parameters of the atoms can be sampled, obtaining a finite dictionary with discrete parameters that is complete and, indeed, capable of representing any signal.

The phase $\phi \in [0,\pi)$ and $K_\gamma$ is such that $||g_\gamma(t)|| = 1$. Sampling $\gamma$ gives [2] $\gamma_s = [2^j, p2^j, k\pi 2^{1-j}, \phi]$, $j,p,k \in \mathbb{Z}$. Thus, $\gamma_s$ can be represented uniquely by $\gamma_s = [j,p,k,\phi] \in \mathbb{Z}^3\times\mathbb{R}$ (the phase is continuous). The index $j$ defines the atom scaling, $p$ defines the time shift, and $k$ defines the atom's modulation. With

$L = \log_2(N)$, the indexes ranges are $j \in [0, L]$, $p \in [0, N2^{-j})$, $k \in [0, 2^j)$ [2]. Thus, the discrete atom $g_{\gamma_s}(m)$ is

$$\begin{aligned} g_{\gamma_s}(m) &= g_j(m - p2^j)\cos(mk\pi 2^{1-j} + \phi) \\ g_j(m) &= \begin{cases} \delta(m), & \text{if } j = 0 \\ K_{\gamma_s} g\left(\frac{m}{2^j}\right), & \text{if } j \in (0, L) \\ \frac{1}{\sqrt{N}}, & \text{if} j = L \end{cases} \\ \text{with } g(m) &= 2^{1/4} e^{-\pi m^2} \end{aligned} \tag{4}$$

where $K_{\gamma_s}$ is equivalent to $K_\gamma$. We do not need to search for the phase $\phi$. It is derived analytically from the triplet $(s, u, \xi)$ (see Section IV-A).

From the discretely parameterized atom, a local search by a pseudo-Newton method [21] can be applied to find a continuous parameters set $\gamma$ that best matches $\mathbf{g}_\gamma$ to the current residue being decomposed. This achieves an MP using a Gabor dictionary with densely sampled parameters. We have implemented and tested both the discrete and "continuous-parameter" versions of the MP. The results were around 10% better (this refers to inner products values), on average, for the continuous case. Thus, when searching for the damped sinusoid, we start from a continuous-parameters Gabor atom. To obtain the continuous-parameter Gabor atom, using the Newton method, there is no closed form for the inner product $\langle \mathbf{x}, \mathbf{g}_\gamma \rangle$; therefore, inner products ought to be calculated for each new update of the atom parameters. Directed by these observations, the strategy employed for the pseudo-Newton method was as follows: **I**) Independently increment each parameter of the atom by half of its value. **II**) If the inner product increases, then the parameter is updated; otherwise, the increment is negated and halved (multiplied by -0.5) for the next iteration. **III**) At each iteration, the three parameters $[s, u, \xi]$ are tested in a sequentially ordered fashion for updates. **IV**) The iterations take place until the inner product increase is less then 1% or the parameter increment is less then 10% of their actual values. Note that when implementing an MP with a continuous-parameter dictionary, the fast MP algorithm [2] (based on correlation updates) is not applicable.

Next, we discuss how to compute the optimum phase $\phi$ for an atom, given the residue. In addition, the suppression of the pre-echo and post-echo artifacts that appear when using the MP is investigated. For other examples of these phenomena, see [2] and [22]. Actually, [22] presents the so-called High Resolution Pursuits (HRPs), which try to overcome the problem by never adding any atoms to the decomposition that would introduce pre-echoes.

### A. Optimum Phase Computation

Once the parameters $(s, \tau, \xi) = \gamma$ are found, the optimum phase for the atom can be computed [5], [23]. The result presented in [23] is for continuous time atoms but can be generalized to discrete ones. Any unit-norm atom depending on a set of parameters $\gamma = (\eta, \xi, \phi)$ is given by

$$g_\gamma(t) = \frac{g_\eta(t)\cos(\xi t + \phi)}{\| g_\eta(t)\cos(\xi t + \phi) \|} \tag{5}$$

where $g_\eta(t)$ can be any real function that depends on the set $\eta$ [for Gabor atoms $\eta = (s, \tau)$, see (7), and for the damped sinusoid $\eta = (\rho, t_s, t_e)$, see (4)]. $g_\gamma(t)$ can be regarded as the real part of a complex function $G_\gamma(t)$, $G_\gamma(t) = g_\eta(t)e^{j\xi t + \phi}$, normalized to have unit energy. Defining $P_\gamma(t) = \mathrm{Re}\{G_\gamma(t)\}$ and $Q_\gamma(t) = \mathrm{Im}\{G_\gamma(t)\}$ at the $n$th step of the MP, the optimum phase $\phi_o \in [0, 2\pi)$ (always obtaining positive inner products) for the atom is given by the following.

1) If $\xi \neq 0$ and $a \neq 0$, and $\left\langle \mathbf{R}^n_{x(t)}, P_{\gamma(n)}(t) \right\rangle / \| P_{\gamma(n)}(t) \|$
$\begin{cases} > 0, & \text{then } \phi_o = \arctan(-b/a) \\ < 0, & \text{then } \phi_o = \arctan(-b/a) + \pi. \end{cases}$
2) If $\xi = 0$ and $-\left\langle \mathbf{R}^n_{x(t)}, Q_{\gamma(n)}(t) \right\rangle / \| Q_{\gamma(n)}(t) \| \begin{cases} > 0, & \text{then } \phi_o = 0 \\ < 0, & \text{then } \phi_o = \phi \end{cases}$.
3) If $a = 0$ and $\left\langle \mathbf{R}^n_{x(t)}, P_{\gamma(n)}(t) \right\rangle a + \left\langle \mathbf{R}^n_{x(t)}, Q_{\gamma(n)}(t) \right\rangle b / \| aP_{\gamma(n)}(t) + bQ_{\gamma(n)}(t) \| \begin{cases} > 0, & \text{then } \phi_o = \pi/2 \\ < 0, & \text{then } \phi_o = 3\pi/2 \end{cases}$

where

$$\begin{aligned} a &= \left\langle \mathbf{R}^n_{x(t)}, P_{\gamma(n)}(t) \right\rangle \| Q_{\gamma(n)}(t) \|^2 \\ &\quad - \left\langle \mathbf{R}^n_{x(t)}, Q_{\gamma(n)}(t) \right\rangle \langle P_{\gamma(n)}(t), Q_{\gamma(n)}(t) \rangle \\ b &= \left\langle \mathbf{R}^n_{x(t)}, Q_{\gamma(n)}(t) \right\rangle \| P_{\gamma(n)}(t) \|^2 \\ &\quad - \left\langle \mathbf{R}^n_{x(t)}, P_{\gamma(n)}(t) \right\rangle \langle P_{\gamma(n)}(t), Q_{\gamma(n)}(t) \rangle. \end{aligned} \tag{6}$$

### B. Pre-Echo and Post-Echo Reduction

When using the MPs to decompose signals, undesirable artifacts of pre-echo and post-echo may arise. As an example, consider the decomposition of the synthetic signal *S1*, which is just the atom corresponding to the six-tuple (1.000, 8, 0.080, -90, 0.0312, 0.1059) (see Section III), with fundamental frequency $F = 60$ Hz [see (3)] and sampling frequency $F_s = 1200$ Hz. The decomposition of *S1* using the discrete parameter Gabor Dictionary with an optimal phase is shown in Fig. 2 at a different number of steps (2, 4, and 8), where pre-echo and post-echo artifacts can be seen.

One way to suppress those artifacts is to include in the dictionary atoms having all possible temporal supports. This is equivalent to box-windowing the atoms as

$$g_{\gamma_l}(t) = K_l \frac{1}{\sqrt{s}} g\left(\frac{t - \tau}{s}\right)\cos(\xi t + \phi)[u(t - t_s) - u(t - t_e)] \tag{7}$$

where $g(t) = 2^{1/4}e^{-\pi t^2}$, and $u(t)$ is the step function. Defining $\gamma_l = (s, \tau, \xi, \phi, t_s, t_e)$ with $t_s < t_e$, where $t_s$ is the starting time of the atom, $t_e$ is its ending time, and $K_l$ is chosen such that $\| g_{\gamma_l}(t) \| = 1$. Finding $t_s$ and $t_e$ that minimize the error norm in the support region of the atom would cope with the pre-echo and post-echo artifacts. For digitized signals, the error norm in the support region, at the step $(n)$, is given by $\mathbf{e}_{[m_s, m_e]} = \| (\mathbf{R}^n_{\mathbf{x}} - \langle \mathbf{R}^n_{\mathbf{x}}, \mathbf{g}_{\gamma_l(n)} \rangle \mathbf{g}_{\gamma_l(n)})[\mathbf{u}(m - m_s) - \mathbf{u}(m - m_e)] \|$, where $m_s$ is the signal sample corresponding to $t_s$, and $m_e$ corresponds to $t_e$ (note that initially, for all the atoms, $m_s = 0$ and $m_e = N - 1$, where $N$ is the signal length). Actually, minimizing the norm of the error is the same as finding the support interval that gives the largest inner product (the atoms with new time support must

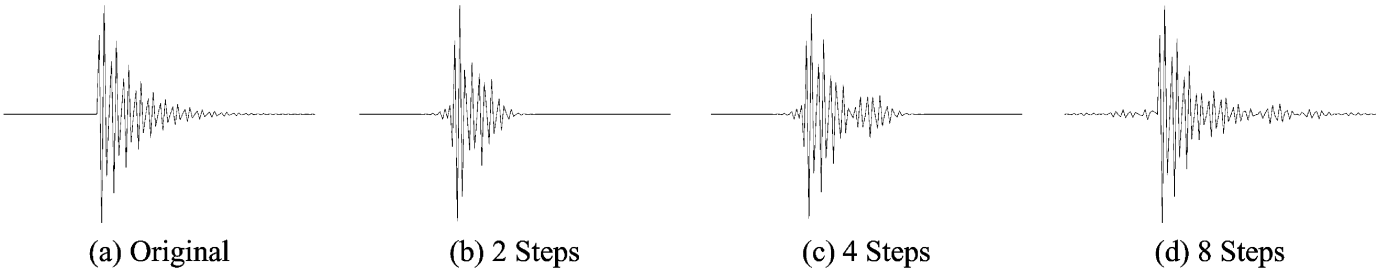


Fig. 2. Reconstructed versions of the synthetic signal *S1* with the MPs of continuous parameters and optimum phase with two, four, and eight steps.

be renormalized to unity norm). Then, a new support interval $[m_s', m_e']$ is considered for the atom only if

$$\left\langle \mathbf{R}_{\mathbf{x}}^n, \mathbf{g}_{\gamma_{l'}(n)} \right\rangle \geq \left\langle \mathbf{R}_{\mathbf{x}}^n, \mathbf{g}_{\gamma_l(n)} \right\rangle \text{ and } m_e' - m_s' < m_e - m_s \quad (8)$$

where $\gamma_{l'} = (s, \tau, \xi, \phi, m_s', m_e')$. That is, the best time support for the atom is the one yielding an inner product that is greater than or equal to the inner product of the atom with larger temporal support for the same $(\gamma, \phi)$. Being $\gamma_l = (s, \tau, \xi, \phi, m_s, m_e)$, it is easy to show that if $\gamma_{l'} = (s, \tau, \xi, \phi, m_s, m_e - 1)$, then

$$\left\langle \mathbf{R}_{\mathbf{x}}^n, \mathbf{g}_{\gamma_{l'}(n)} \right\rangle = \frac{\left\langle \mathbf{R}_{\mathbf{x}}^n, \mathbf{g}_{\gamma_l(n)} \right\rangle - R_{\mathbf{x}}^n(m_e) g_{\gamma_l(n)}(m_e)}{\sqrt{1 - g_{\gamma_l(n)}^2(m_e)}} \quad (9)$$

where $R_{\mathbf{x}}^n(m_e)$ is the $m_e$th sample of $\mathbf{R}_{\mathbf{x}}^n$, and $g_{\gamma_l(n)}(m_e)$ is the $m_e$th sample of $\mathbf{g}_{\gamma_l(n)}$. Thus, if we know the inner product in (8) for a given value of $m_e$, the inner products for smaller values of $m_e$ can be computed recursively and, consequently, with low computational complexity. A similar result tells us that an inner product for an atom starting at $m_s + 1$ can be computed from the one of the atom starting at $m_s$. In addition, in order to further simplify this procedure, the search can be performed independently for $m_s'$ and $m_e'$, leading to a fast algorithm to find the best time support.

Fig. 3 shows the reconstruction of synthetic signal *S1* for a four-step decomposition without and with temporal support search in the continuous-parameter Gabor dictionary. When temporal support search is applied, the reconstructed signal is visibly more similar to the original one, and the pre-echo and post-echo artifacts vanish in this example; differences are noticed only after the 80th sample, where the signal has little energy. When decomposing this signal with the Gabor dictionary of discrete parameters and optimum phase, we obtain an inner product at the first step of 1.643, whereas using the continuous parameters, it jumps to 2.0874 (a 27% increase). Further performing the search for the best time support, the result becomes 2.145 (around 3% increase to the second and 30% increase to the former). Since the energy of the signal is equal to the sum of the energies of the inner products [4], a larger inner product means a smaller reconstruction error. This shows that the closer visual similarity corresponds to a closer match in a mean-squared sense.

Here, unlike standard MP algorithms where the set of structures is static (discrete parameters and fixed dictionary), we have obtained an MP with a dictionary of continuous parameters. In addition, the structures found have the best time support, eliminating pre-echo and post-echo artifacts.

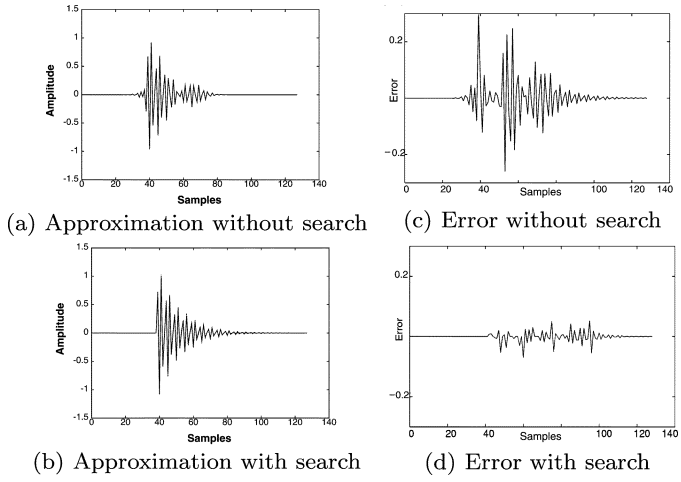


Fig. 3. Synthesis of synthetic signal *S1* [Fig. 2(a)] after decomposition using four steps of the *MPs* with densely sampled *Gabor* dictionary. (a) and (c) Without and (b) and (d) with the temporal support search of Section IV-B.

## V. Signal Decomposition Using MP With Damped Sinusoids Dictionary

In the proposed approach, an indirect search for the damped sinusoids is carried out. First, the continuous-parameter Gabor atom that maximizes the inner product is found. These parameters are then used to generate a guess for the best damped sinusoid. This guess initializes a pseudo-Newton algorithm to find the parameters of the best damped sinusoid. When we perform such indirect damped sinusoid search, one cannot use correlation updates (as in [2]), and therefore, there is no fast MP algorithm. This is because the dictionary we effectively use has continuous parameters and, thus, infinite cardinality. Therefore, the computational complexity of the proposed method is increased when compared with the one of the standard MP; however, the good results obtained justify the increase in complexity.

### A. Search for the Damped Sinusoids

The procedure to obtain the damped sinusoid that is best represented at step $n$ of the MP is the following.

1) Find the Gabor atom index $\gamma = [s, \tau, \xi, \phi_o]$ such that $\gamma = \arg\{\max_{\gamma \in \Gamma} |\langle \mathbf{R}_{\mathbf{x}}^n, \mathbf{g}_\gamma \rangle|\}$ using the MP with optimum phase (see Section IV-A).
2) Obtain the initial guess for the damped sinusoid:
   a) Find the half plane of the Gabor atom above that has a higher inner product with the signal: Either the right half (defined as the points to the right of the Gaussian window center $\tau$), which implies a decreasing exponential to be searched for, or the left half (defined as

the points to the left of the Gaussian window center $\tau$), which implies an increasing exponential to be searched for. That is, the best half-plane is the Gabor atom's half with a higher inner product with the current residue.

b) With the scale $s$ found, compute the initial guess for the damping factor $\rho$ that best matches the half-plane identified above. This initial value is given by $\rho = \sqrt{\pi/2s^3}$ for a decreasing exponential and $-\sqrt{\pi/2s^3}$ for an increasing exponential. This value of $\rho$ leads to the damped sinusoid having the same sample value of the Gaussian at its inflection point. In case of functions with limited time support, this value needs to be corrected. This is done iteratively by a pseudo-Newton algorithm (fast and in closed-form as both functions are known).

c) With the obtained $\rho$, $\tau$, and $\psi$ previously found, a pseudo-Newton method is applied to search for the atom $\mathbf{g}(m) = K_g e^{-\rho(m-m_s)} \cos(\pi\xi m + \phi)[\mathbf{u}(m - m_s) - \mathbf{u}(m - m_e)]$, where $K_g$ is a normalization factor. As the modulated exponential can be increasing or decreasing ($\rho > 0$ or $\rho < 0$), we must devise how to search for the start and end samples of the damped sinusoid. In the case of a decreasing exponential, we assume that $m_s = \tau$ and that $m_e = N - 1$. In the case of an increasing exponential, $m_s = 0$, and $m_e = \tau$. A pseudo-Newton algorithm is applied to obtain one of the five-tuples $\gamma = [\rho, \xi, \phi, \tau, N-1]$ or $\gamma = [\rho, \xi, \phi, 0, \tau]$ ($\tau$ can represent either the start or end time). The phase is obtained through the procedure of Section IV-A. The pseudo-Newton method applied is similar to that presented for the Gabor atom (see Section IV) but for four parameters $[\rho, \xi, \phi, \tau]$ (with the same constraints: step computation, and stop criterion).

3) Search for the best time support, as in Section IV-B, obtaining the five-tuple $\gamma = [\rho, \xi, \phi, m_s, m_e]$ that characterizes the atom. Note the following: **a**) If $\rho > 0$, then we have a decreasing atom, and we must search only for $m_e$. **b**) If $\rho < 0$, then the atom is an increasing one, and the time support search must be done for $m_s$.
4) For the best time support found above, make a new local search for $\rho$ and $\xi$ using the pseudo-Newton method, and compute $\phi$.
5) With the five-tuple $\gamma = [\rho, \xi, \phi, m_s, m_e]$, we compute the inner product of the corresponding atom with the current residue $\langle \mathbf{R}_{\mathbf{x}}^n, \mathbf{g}_\gamma \rangle$, and the process is finished.

In the search process, we end up with damped sinusoids, as in (3), which can have any phase $\phi$. These atoms are called dereferenced [5] as the atoms' start time and phase are not related.

The identification of damped sinusoids using this approach performed effectively. An illustration of this effectiveness will be given in Section VII, where results with natural signals are shown.

### *B. Frequency Quantization*

The decomposition obtained represents a signal as a sum of damped sinusoids of any frequencies. To obtain the proposed signal model, the frequencies of the structures must be quantized as integer multiples of the fundamental frequency. The quantization process must take into account the sampling frequency $F_s$ (the maximum possible frequency in the signal is $F_s/2$). The frequency quantization can then be performed as follows:

1) Compute the ratio between the sampling frequency and the fundamental $r_f = F_s/F$.
2) With this ratio, design a quantizer for the frequency of the atom $\xi$ using a linear quantizer of $b_{q(\xi)} = \lceil \log_2 r_f \rceil$ bits and step $\Delta_{q(\xi)} = \pi/2^{b_{q(\xi)}}$.
3) The quantized frequency for an atom is $\xi_q = \lfloor \xi + (\Delta_{q(\xi)}/2)/\Delta_{q(\xi)} \rfloor \times \Delta_{q(\xi)}$, where $\xi$ is the original frequency of the atom.
4) After quantizing the frequency, a local optimization using the pseudo-Newton method is performed for the damping factor $\rho$.

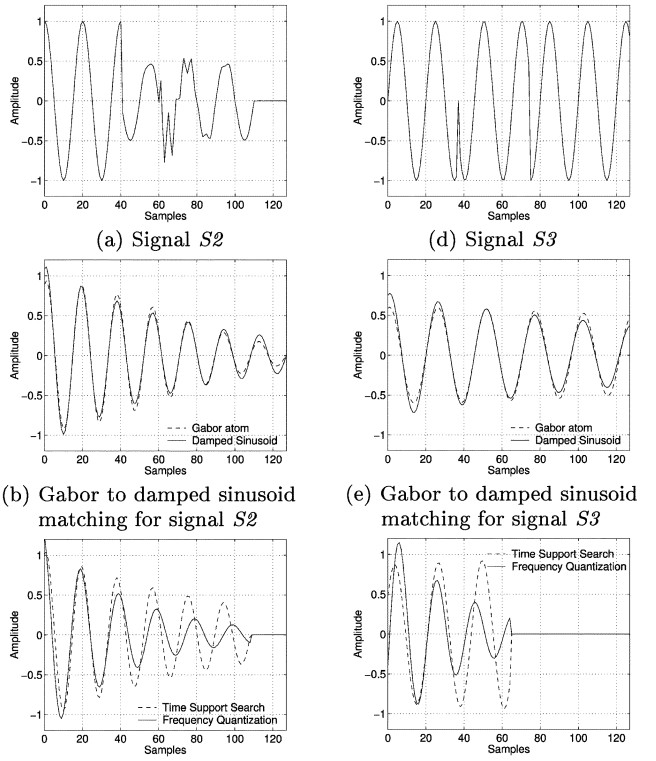


(a) Signal *S2* (d) Signal *S3*

(b) Gabor to damped sinusoid matching for signal *S2* (e) Gabor to damped sinusoid matching for signal *S3*

(c) Time support search and frequency quantization for signal *S2* (f) Time support search and frequency quantization for signal *S3*

Fig. 4. First-step decomposition of synthetic signals *S2* and *S3* with time support search and frequency quantization.

Some examples are shown in order to point out problems regarding the identification of structures. In Fig. 4, we can see the described process behavior at the first step of the decomposition of synthetic signals *S2* in Fig. 4(a) and *S3* in Fig. 4(d), whose parameters are given in Table I (where $m_{s_q}$ and $m_{e_q}$ are the samples indexes of $t_{s_q}$ and $t_{e_q}$, respectively, and $q$ is the component number). These synthetic signals were chosen as they are representative of common phenomena in power systems [1], [14], [16], [18], [19], [24], [25]. Indeed, they indicate the limitations of the MP algorithm and the effectiveness of the procedures presented for the desired application. In Fig. 4(b), we can observe the damped sinusoid obtained from the Gabor atom guess that best matches the signal *S2* [see Fig. 4(a)]. In Fig. 4(c), we can observe the result of the time support search for the damped sinusoid atom and frequency quantization. The same is presented for signal *S3* in Fig. 4(e) and (f), respectively. Note that prior

TABLE I
GENERATION OF THE SYNTHETIC SIGNALS *S2*, *S3*, AND *S4* ACCORDING TO THE MODEL OF (3)

| Signal | $F_s$ (Hz) | $F$ (Hz) | $A_q$ | $k_q$ | $\phi_q$ (Deg.) | $\rho_q$ | $t_{s_q}$ (Sec.) | $t_{e_q}$ (Sec.) | $m_{s_q}$ | $m_{e_q}$ |
|---|---|---|---|---|---|---|---|---|---|---|
| *S2* | 1200 | 60 | 1.000 | 1 | 0 | 0 | 0 | 0.0333 | 0 | 40 |
| | | | 0.500 | 1 | 90 | 0 | 0.0333 | 0.0917 | 40 | 110 |
| | | | 0.200 | 6 | -90 | 0.100 | 0.0500 | 0.1059 | 60 | 127 |
| | | | 0.050 | 3 | -67 | 0 | 0.0417 | 0.0833 | 50 | 100 |
| *S3* | 1200 | 60 | 1.000 | 1 | -90 | 0 | 0.0625 | 0.1059 | 75 | 127 |
| | | | 1.000 | 1 | -90 | 0 | 0 | 0.0308 | 0 | 37 |
| | | | 1.000 | 1 | 135 | 0 | 0.0308 | 0.0625 | 37 | 75 |
| *S4* | 1500 | 50 | 1.000 | 1 | 0 | 0 | 0 | 0.0200 | 0 | 30 |
| | | | 0.250 | 2 | 90 | 0.1 | 0.0200 | 0.0533 | 30 | 80 |
| | | | 0.100 | 6 | 68 | -0.03 | 0.0447 | 0.0847 | 67 | 127 |

to frequency quantization, the frequency of the decomposing structure is different from the original one used to generate the signal component. The frequency quantization effectively corrects this error, which is caused by the greediness of the MP decomposition together with the particularities of the dictionary used. Although this behavior may seem odd, the atom found prior to quantization is the one with higher inner product with the signal under decomposition. Indeed, as we have observed through simulations, even by forcing the frequency of the decomposing structure to be equal to the one used in generating the atom, the inner product is still smaller than the one found by the decomposition algorithm. In the present case, we ideally want to find the three structures that, when concatenated, give the largest inner product with the signal.

As observed in these examples, the searches for damped sinusoids and frequency quantization perform well. Still, some false phenomena identification takes place due to the greedy aspect of the MP.

1) Signals formed by two or more sinusoids of same phases but different amplitudes are confused as one damped sinusoid, as is the case of the decomposition of signal *S2* in Fig. 4(b). Signal *S2* is formed by two sinusoids of same phases: one of them being corrupted by higher frequency components. However, the damped sinusoid chosen by the MP to represent the signal is a decreasing exponential almost in phase with the higher energy sinusoid with full time support. Note that the amplitude decrease at the 40th sample is not identified.
2) Sinusoids of the same frequency and amplitude but different phase are identified as one sinusoid with phase that maximizes the inner product. That is exactly the case of signal *S3*, with two phase discontinuities, which are usually caused by switching, for which the 90° phase change (around the 70th sample) is located by the time support search, but the smaller phase change (around the 40th sample) is not.

In fact, the false phenomena identification that take place when decomposing signals with greedy approximation algorithms have previously been described in [26] (see Section IV). There, the authors give an example of a signal composed by a sum of two dictionary structures in which these structures could not be found by the greedy decomposition. In Section V-D, an algorithm is proposed that obtains better structure identification for the signal model proposed here and addresses the limitations presented above.

### C. Complexity Issues

In this subsection, we will discuss computational complexity issues of the proposed method.

Due to the nature of the problem at hand, we can use frequency quantization. This contributes to decreasing the computational complexity since it represents a significant decrease in size of the search space, and the sinusoids generated by these quantized frequencies can be either precomputed or generated on the fly using efficient algorithms as the fast Fourier transform (FFT).

One important point affecting the computational complexity is that the recurrent formula for fast computation of the MP, as in [2], is not applicable to the present case. This is so because at the end of each decomposition step, the signal is decomposed by an atom from a dictionary that has infinite cardinality (continuous parameters), which makes it impossible to prestore all the inner products between the dictionary atoms; therefore, the recurrence relation in [2] cannot be used.

In addition, the continuous-parameter dictionary requires the use of a Newton method at each iteration, leading to high computational demands. Actually, the Newton method in a multivariate space is used twice: one for finding the best Gaussian atom (see Section IV) and the other for finding the best damped sinusoid (see Section V-A). It is important to note that the use of a discrete-parameter dictionary followed by a Newton method in order to generate a continuous parameter dictionary has often been suggested in the literature [2]. In addition, note that for signals of length $N$, if we used a dictionary with discrete parameters, its cardinality would be $2^{b_{q(\xi)}} \times A \times N(N-1)$, where $2^{b_{q(\xi)}}$ is the number of quantized frequency levels, $A$ is the number of different possible damping factors $\rho$, and $N(N-1)$ is the number of all possible time-support intervals. Note that to use a dictionary with such a cardinality is prohibitive (the initial discrete Gabor dictionary has cardinality $\log_2(N)N$, i.e., much smaller than previously for any $2^{b_{q(\xi)}} \times A$); therefore, taking into consideration the fact that a continuous-parameter dictionary has superior performance (see the end of Section IV-B), its use is clearly a viable alternative.

### D. Pure Sine Substitution

The structures found in the examples in Section V-B, despite leading to the largest inner product with the signal, do not match the phenomena represented in it. This problem is inherent to any MP-based or greedy decomposition [26]. To solve this, the component that we chose to represent the atom, which is either a damped or a pure (or plain) sinusoid, will be the one that

gives smaller error in the region of support of the atom (this is closer to a shape similarity measure than the inner product). Previous works have shown that a successful representation relies on detailed analysis or an appropriate distortion model in order to select the atoms [27], [28]. The proposal is similar to the criterion of Section IV-B, with extra conditions on the inner product. There are two cases in which we will use a pure sinusoid instead of a damped one of the same frequency. These cases are supported by the assumption that, as in traditional works on MP [2], [4], a fraction (close to one) of the maximum inner product is acceptable for selecting the atom to represent the residue at a given step. However, in our case, this fraction is only acceptable, provided that a shape similarity measure (the error per sample) is satisfied in a given region. Considering two sets of parameters $\gamma(n) = (k, \rho, \phi, m_s, m_e)$ (damped sinusoid) and $\gamma'(n) = (k, 0, \phi, m'_s, m'_e)$ (pure sinusoid), where $\mathbf{R}^n_{\mathbf{x}}$ is the current residue, the cases are as follows.

- **i**) If the inner product of the pure sinusoid with the signal is at least $p_1$ times the inner product $(0 < p_1 < 1)$ obtained with the damped sinusoid, then use the pure sinusoid. That is, if $|\langle \mathbf{R}^n_{\mathbf{x}}, \mathbf{g}_{\gamma'(n)} \rangle| \geq p_1 |\langle \mathbf{R}^n_{\mathbf{x}}, \mathbf{g}_{\gamma(n)} \rangle|$, then use $g_{\gamma'(n)}$ instead of $g_{\gamma(n)}$ to represent the current residue.
- **ii**) If the inner product of the pure sinusoid with the signal is greater than $p_2$ times the inner product $(0 < p_2 < p_1 < 1)$ obtained with the original damped sinusoid, then we verify if a pure sinusoid should be used to represent the signal (see 1 and 2 below). More precisely, if case **i** above is not satisfied and $|\langle \mathbf{R}^n_{\mathbf{x}}, \mathbf{g}_{\gamma'(n)} \rangle| \geq p_2 |\langle \mathbf{R}^n_{\mathbf{x}}, \mathbf{g}_{\gamma(n)} \rangle|$, then it should be verified whether it is worthwhile to use $g_{\gamma'(n)}$ instead of $g_{\gamma(n)}$ to represent the signal at the step.

  Case **i** is straightforward since the use of a pure sinusoid will be only slightly worse, in terms of energy reduction, than the use of the damped one. In case **ii**, the use of the pure sinusoid is significantly worse than the damped one, but it is still valuable to verify the possibility of using a pure sinusoid instead of the damped one. Obviously, these impose $p_1 > p_2$. Simulations on a large set of natural and synthetic signals have suggested for $p_1$ the value 0.99 and for $p_2$ the value 0.75. In brief, if case **i** is met, a pure sinusoid will be used; otherwise, a pure sinusoid will be searched for to represent the current residue if case **ii** holds. This is done as follows:

1) From the frequency and the temporal limits (in samples) of the structure, a region in which to search for a possible pure sinusoid to represent the signal is computed by defining $\Delta_T = F_s/F$ [$F$ is the fundamental frequency; see (5)]. The limits of the region where the pure sinusoid may be located are then given by $m'_s = m_s - \Delta_T/2$ and $m'_e = m_e + \Delta_T/2$. This range yields a possible region of support that is one cycle larger than the one of the original atom (half cycle before the start and half cycle after the end of the structure).
2) A pure sinusoid $g_{\gamma'(n)}$ $(\rho = 0)$ of the same frequency as the damped one $g_{\gamma(n)}$ will be a candidate to represent the signal at the current step in the region of support $[m_s - (\Delta_T/2),\ m_e + (\Delta_T/2)]$ if the two conditions below hold simultaneously:
   a) The error per sample in the region of support for the pure sinusoid is smaller than the error per sample for the damped sinusoid in the region of support of the pure sinusoid. That is, we have (10), shown at the bottom of the page, where the primed variables correspond to the pure sinusoid and the nonprimed ones to the damped sinusoid. This error-per-sample metric is intended to avoid modeling errors that would have to be corrected in later iterations of the MP algorithm. Equation (10) compares the pure to the damped sinusoid in the region where the first is defined, providing a shape similarity measure in this region. As in the case of the pre-echo and post-echo suppression, which is described in Section IV-B, the expression in (10) can be computed recursively in a fast fashion.
   b) The error per sample for the pure sinusoid is smaller than or equal to half of the error per sample obtained with the damped sinusoid in its original region of support, that is, we have (11), shown at the bottom of the page. This procedure compares the overall shape similarity of the two possible atoms in their respective regions of support. We also impose the inner product of the current residue with the pure sinusoid to be at least 50% of what is obtained with the damped sinusoid. This constraint forces a reasonable and acceptable approximation ratio in the step.

Note that the search for the best time support can be performed independently for $m_s$ and $m_e$. If $\rho > 0$, then it is expected that the start time of the atom is well defined since this is the region of the structure with largest energy. Thus, we first search for $m_e$ by applying the two conditions above, and then, we search for $m_s$ using the same conditions. In the case where we have $\rho < 0$, $m_e$ is expected to be well defined, and then, we first search for $m_s$ and then for $m_e$.

$$\frac{\left\| \left( \mathbf{R}^n_{\mathbf{x}} - \left\langle \mathbf{R}^n_{\mathbf{x}}, \mathbf{g}_{\gamma'(n)} \right\rangle \mathbf{g}_{\gamma'(n)} \right) \left[ \mathbf{u}(m - m'_s) - \mathbf{u}(m - m'_e) \right] \right\|}{m'_e - m'_s - 1} < \frac{\left\| \left( \mathbf{R}^n_{\mathbf{x}} - \left\langle \mathbf{R}^n_{\mathbf{x}}, \mathbf{g}_{\gamma(n)} \right\rangle \mathbf{g}_{\gamma(n)} \right) \left[ \mathbf{u}(m - m'_s) - \mathbf{u}(m - m'_e) \right] \right\|}{m'_e - m'_s - 1} \tag{10}$$

$$\frac{\left\| \left( \mathbf{R}^n_{\mathbf{x}} - \left\langle \mathbf{R}^n_{\mathbf{x}}, \mathbf{g}_{\gamma'(n)} \right\rangle \mathbf{g}_{\gamma'(n)} \right) \left[ \mathbf{u}(m - m'_s) - \mathbf{u}(m - m'_e) \right] \right\|}{m'_e - m'_s - 1} \leq \frac{\frac{1}{2} \left\| \left( \mathbf{R}^n_{\mathbf{x}} - \left\langle \mathbf{R}^n_{\mathbf{x}}, \mathbf{g}_{\gamma(n)} \right\rangle \mathbf{g}_{\gamma(n)} \right) \left[ \mathbf{u}(m - m_s) - \mathbf{u}(m - m_e) \right] \right\|}{m_e - m_s - 1}. \tag{11}$$

In Fig. 5, this algorithm is verified when applied to the first step of the decompositions of signals *S2* and *S3*. Fig. 5 presents the sine discrimination together with the quantized frequency-damped sinusoid identified so far (see Fig. 4). Note that the pure sinusoidal structures found are totally coherent to the structures used to generate the atoms. Thus, the proposed sine discrimination procedure succeeded in correcting the erroneous decisions made by the MP algorithm. We have verified that this procedure does not impact the cases where the damping is representative of the phenomenon, as will be seen in examples to be shown.

Summarizing, the full decomposition algorithm (shown in Fig. 1) and reconstruction consists of the following steps:

1) Apply one step of the decomposition:
   a) Carry out one step of the MP algorithm with the Gabor Dictionary.
   b) From the obtained Gabor atom, search for a damped sinusoid (Section V-A).
   c) Quantize the structure frequency (Section V-B).
   d) Apply the sine substitution heuristic (Section V-D).
2) Repeat (2) iteratively until some stop criterion such as a fixed number of steps or a prescribed error is met or by using the criterion to be presented in Section VI.
3) Reconstruct the signal with these structures.

Using the procedures described, the atoms found are physically meaningful (refer to Figs. 4–6). This can be confirmed by the decomposition of signal *S4* [see Fig. 6(a)]. The structures identified for that signal, using a three-step decomposition, are presented in Fig. 6(b), and the reconstructed signal in shown Fig. 6(c). In Table II, the parameters of the structures extracted by the decomposition algorithm for signals *S3* and *S4* are shown together with the parameters used to generate them. Signal *S4* is reconstructed with an SNR of 29.79 dB and signal *S3* with an SNR of 92.87 dB (SNR is defined in Section VII, (14)), implying that the estimation of the structure parameters is accurate for these signals. The results shown so far aim to verify the proposed method's behavior with completely known signals and are not intended to serve as arguments for its validation. A convincing validation of the proposed method can only be performed by decomposing natural signals; this is addressed in Section VII.

### E. Application to Filtering of DC Components

Here, we show a study on the capability of the MP in filtering the exponential decay that sometimes appears in current quantities after disturbances, which are commonly known as the "DC Component" [29]. It appears to be added to the sinusoid and can be modeled as $Ae^{-\lambda t}[u(t-t_s)-u(t-t_e)]+B\sin(2\pi Ft+\phi)$, where $t_s$ and $t_e$ are the start and end times of the phenomenon (for simplicity, the start and end times of the sinusoidal component are not presented), and $\lambda$ is the exponential decay constant. Observe that this is a particular case of (3), and we expect that the decomposition developed is capable of extracting/identifying the "DC Component." Once the signal is decomposed, the "DC Component" can be filtered out at the reconstruction process. Furthermore, all the low structures in the signal decomposition that are not of impulsive nature (time support not smaller than 10% of the fundamental frequency period) are eliminated in the reconstruction process. This filtering was effective when applied to synthetic and natural signals as well as signals obtained through the Alternative Transients Program/Electromagnetic Transients Program (ATP-EMTP) [30].

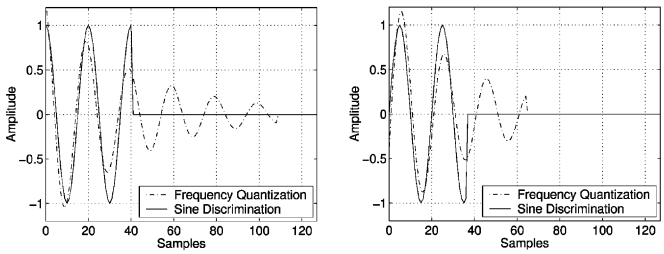


(a) Sine substitution for *S2* (b) Sine substitution for *S3*

Fig. 5. Sine substitutions at the first step decomposition of synthetic signals *S2* and *S3*.

Most analyses of oscillographic signals are based on comparisons of the values of current and voltage quantities, often in phasor form. For that, the signal is filtered to obtain just the fundamental frequency contribution [29]. Therefore, this measure was used to evaluate the proposed filtering. In all cases, the proposed filtering worked very well, and the modulus and angle of the phasor have been correctly estimated. The results for an ATP-EMTP generated signal are shown in Fig. 7. Note that the only significant difference appears in the angle of the phasor after the elimination of the fault; however, in this region, the phasor is null, and this difference is not meaningful. Thus, we see that the modulus variation due to the "DC Component" has been filtered without compromising the angle analysis.

## VI. Coherent Representations With Damped Sinusoids

In previous sections, we have devised a method to decompose an electric signal into coherent components. However, when a given structure is identified, is it really necessary to represent the signal? Does the structure represent signal or noise? These questions are now addressed.

### A. Approximation Ratio

The *Approximation Ratio*

$$\lambda\left(\mathbf{R}_{\mathbf{x}}^{n}\right)=\parallel\langle\mathbf{R}_{\mathbf{x}}^{n},\mathbf{g}_{\gamma(n)}\rangle\parallel/\parallel\mathbf{R}_{\mathbf{x}}^{n}\parallel$$

is a measure of how much of the signal residue is approximated at step $n$ [2], [6]. Fig. 8(a) shows the behavior of the approximation ratio $\lambda\left(\mathbf{R}_{\mathbf{x}}^{n}\right)$ with a Gabor dictionary of discrete parameters and continuous phase (see Section IV) for signals of 128 samples. The values shown are for synthetic signals (presented in Section V) and for a noise signal (denoted as *g-128*) generated with independent identically distributed (i.i.d.) random Gaussian variables. The approximation ratio tends to be inside a neighborhood of a fixed value $\lambda_0$ for a sufficiently large number of steps (although the behavior around this neighborhood is quite irregular) [4]. It should be noted that $\lambda_0$ is independent of the signal being decomposed; it depends only on the dictionary [4], [6], [13]. The dictionary, in turn, depends only on the signal space dimension (length) in our algorithm, as the parameter space of the structures that compose the dictionary is parameterized based only on the signal length. We can also note that for the noise signal (i.i.d. Gaussian noise), the approximation ratio wanders around $\lambda_0$, even at the initial steps. Davis [6], [13] defines the structures with large $\lambda\left(\mathbf{R}_{\mathbf{x}}^{n}\right)$ as the coherent structures since they are

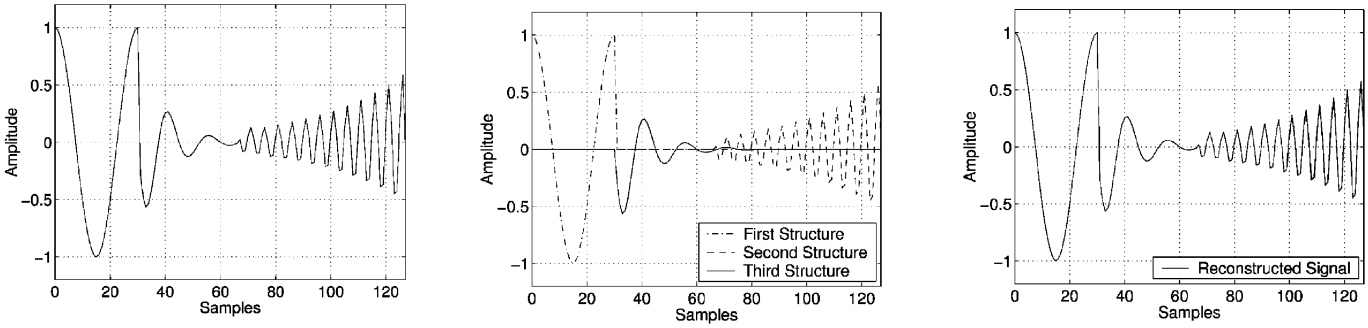


(a) Signal *S4* (b) Structures identified for signal *S4* (c) Reconstructed signal *S4*

Fig. 6. Three steps decomposition of synthetic signals *S4*.

TABLE II
DECOMPOSED STRUCTURES PARAMETERS OF SIGNALS *S3* AND *S4*

| Signal | Atoms Parameters for Signal *S3* | | | | | Atoms Parameters for Signal *S4* | | | | |
|---|---|---|---|---|---|---|---|---|---|---|
| | $\xi$ (Hz) | $\phi$ | $\rho$ | $n_s$ | $n_e$ | $\xi$ (Hz) | $\phi$ | $\rho$ | $n_s$ | $n_e$ |
| Decomposition | 60.00 | 270.00 | 0.00 | 0 | 36 | 50.00 | 0.00 | 0.00 | 0 | 30 |
| | 60.00 | 171.00 | 0.00 | 38 | 74 | 300.00 | 292.67 | -0.029423 | 67 | 127 |
| | 60.00 | 270.00 | 0.00 | 75 | 127 | 100.00 | 90.00 | 0.100022 | 31 | 80 |
| Generation | 60.00 | -90.00 | 0.00 | 0 | 37 | 50.00 | 0.00 | 0.00 | 0 | 30 |
| | 60.00 | 135.00 | 0.00 | 37 | 75 | 300.00 | 68.00 | -0.03 | 67 | 127 |
| | 60.00 | -90.00 | 0.00 | 75 | 127 | 100.00 | 90.00 | 0.1 | 30 | 80 |

highly correlated with the signal. Therefore, one can assume that the residues of the signal being decomposed behave as noise after their approximation ratio is in the vicinity of $\lambda_0$. Thus, if the approximation ratio of the residues behaves like the one of noise, then there are no more coherent components to the dictionary in the residue, and the decomposition/approximation process can be stopped.

Note in Fig. 8(a) the small oscillations around a neighborhood for large values of the step $n$ compared to the values at the initial steps. To filter out the oscillations around $\lambda_0$, we can consider the $L$-step forward mean approximation ratio

$$\lambda_{\text{mean}_f}\left(\mathbf{R}_{\mathbf{x}}^{M}\right) = \frac{1}{L}\sum_{n=M}^{M+L-1}\frac{\| \langle \mathbf{R}_{\mathbf{x}}^{n}, \mathbf{g}_{\gamma_n} \rangle \|}{\| \mathbf{R}_{\mathbf{x}}^{n} \|}. \tag{12}$$

For a given step $M$, if the moving mean approximation ratio in the next $L$ steps is similar to the value of the noise signal mean approximation ratio, we can assume that we are approximating noise. In other words, to avoid modeling such noise, the decomposition should be carried out only while

$$\lambda_{\text{mean}_f}\left(\mathbf{R}_{\mathbf{x}}^{M}\right) \geq \lambda_0 + \varepsilon \tag{13}$$

where $\lambda_0$ is obtained for i.i.d. Gaussian noise signals, and $\varepsilon$ is a confidence constant. Thus, we need to compute, for each dictionary, the mean approximation ratio of the i.i.d Gaussian noise. In Fig. 8(b), we see the behavior of the mean approximation ratio for different length i.i.d Gaussian noise signals of zero mean and unit variance. See that the value of $\lambda_0$ depends on the dictionary (that in this case is completely specified by the signal dimension), which is in agreement with [2], [6], and [13]. When the time support search is applied (see Section IV-B), the approximation ratio changes because it is an intrinsic characteristic of the dictionary for a given signal dimension $N$. Time support search is equivalent to using a much larger dictionary that is composed by the original Gabor dictionary and all its atoms with all possible time supports. This increases the approximation ratio in the step [the search for best time support implies a greater than or equal to inner product; see (13)]. However, it should be observed that with time support search, the values obtained for $\lambda_0$ without this search can still be used as a lower limit for the approximation ratio as a halting criterion. In the results presented in this work, $\varepsilon$ was 10% of $\lambda_0$.

### *B. Approximation Ratio in the Damped Sinusoids Dictionary*

We carry out the MP while the approximation ratio satisfies (13). This guarantees that the MP yields a model consisting of the structures coherent to signal phenomena and not noise components. Table III shows, for the dictionary of damped sinusoids, the values of $\lambda_0$ that are used as the stopping criterion on the decomposition. Note that the damped sinusoid dictionary employed here is fully specified by its dimension, and therefore, the approximation ratio is a function only of the dimension of the signal space. Note that this is independent of the fact that we use the Gaussian-to-damped sinusoid fitting and the procedure to decide whether to use either a pure or a damped sinusoid since every outcome of the five-tuple $(k_q F, \rho, \phi, m_s, m_e)$ is possible.

The values in Table III are for the decomposition using the dictionary of damped sinusoids without frequency quantization and sine discrimination. As these operations decrease the inner products, they tend to reduce the approximation ratio at the decomposition step. Therefore, a small modification in the computation of the approximation ratio in the iteration was performed: The approximation ratio is computed before the frequency quantization and pure sinusoid discrimination. Experimental results showed that this strategy performs well in identifying the coherent structures of the signal. For example, for signals *S2* and *S3*, this procedure identified four and 17 structures, respectively, with an SNR for the reconstructed signals of 83.37 and 93.62 dB, respectively, using $L = \log_2 N$ steps to compute the mean approximation ratio. Nevertheless,

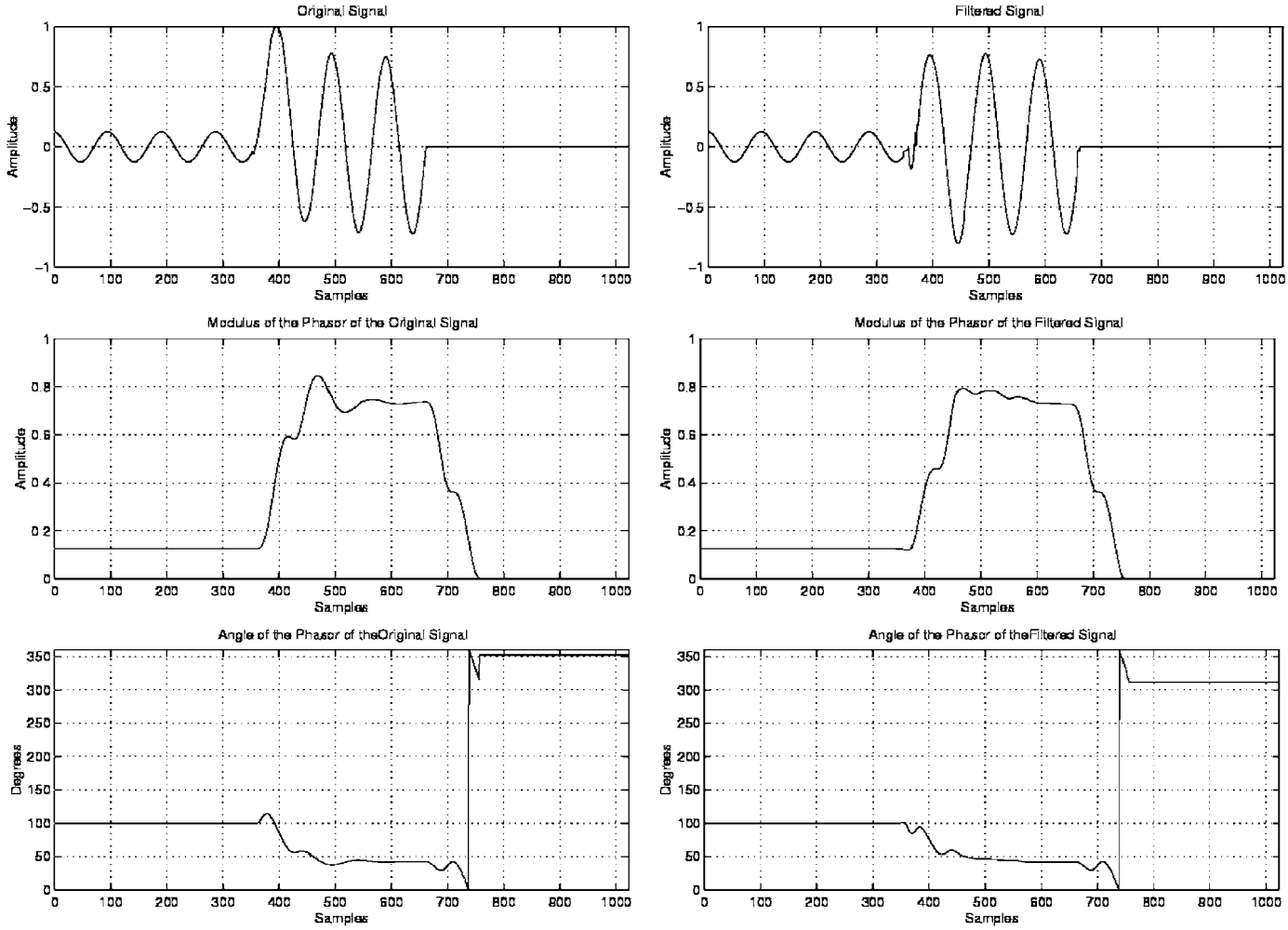


Fig. 7. Fundamental frequency contribution after the "DC Component" filtering of a signal simulated with ATP-EMTP.

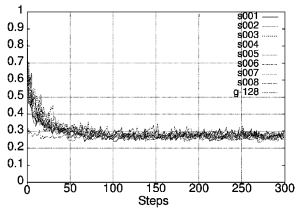


(a) Approximation ratio for signals of size 128.

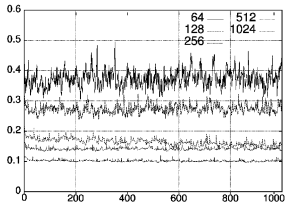


(b) $\lambda_{\text{mean}_f}(\mathbf{R}_{\mathbf{x}}^M)$, Eq. (12), for different signal lengths $N$ $(L = \log_2 N)$.

Fig. 8. Approximation ratio behavior of the MP using the discrete Gabor parameters dictionary with continuous phase.

TABLE III
MOVING MEAN APPROXIMATION RATIO FOR DIFFERENT SIZE NOISE SIGNALS IN THE MP WITH THE DAMPED SINUSOID DICTIONARY OF CONTINUOUS PARAMETERS OBTAINED INDIRECTLY FROM THE MP WITH GABOR ATOMS

| Signal Dimension | 64 | 128 | 256 | 512 | 1024 |
|---|---|---|---|---|---|
| $\lambda_0$ | 0.41 | 0.30 | 0.22 | 0.17 | 0.07 |

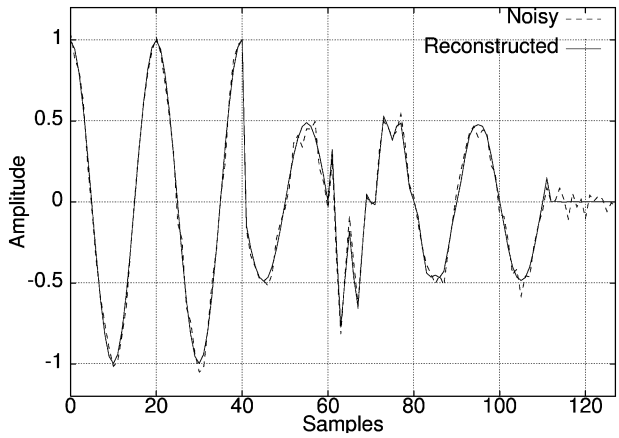


Fig. 9. Decomposition of synthetic signal S2 with noise addition in the damped sinusoid dictionary. The noisy signal is the dashed line, whereas the reconstructed one is in the continuous line.

it is important to point out that most of the structures found have amplitude near zero $(A_q \approx 0)$ that tend to be eliminated during quantization, as will be discussed in Section VII. Note that finding a large number of structures is inherent to the decomposition of most signals (either synthetic or natural) with the MP algorithm. This is so because, since the dictionary is overcomplete, each additional step of the MP can reintroduce components removed in a previous iteration. This tends to generate decompositions with many small energy structures. Solutions to this problem have been proposed. One example is the Orthogonal Matching Pursuits (OMPs) [6], [31].

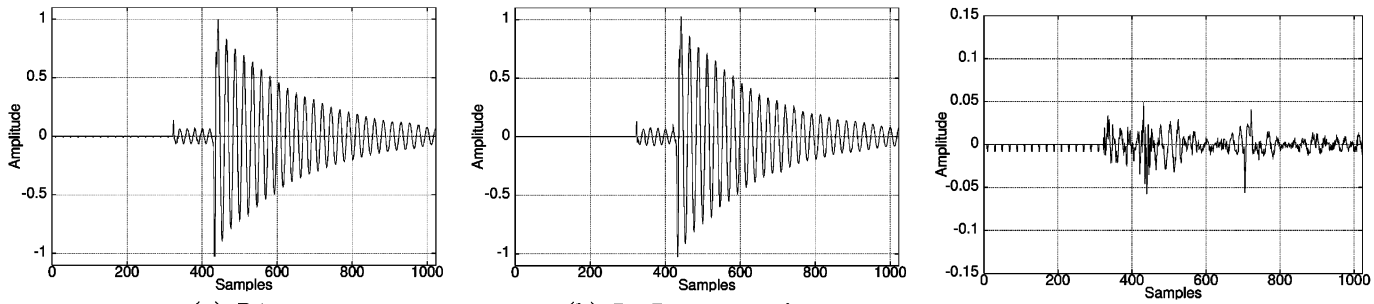


Fig. 10. Quantization of signal R1 with $b_A = 6$, $b_\rho = 7$, and $b_\phi = 7$, where the compression ratio is 15.46, and the SNR is 28.08 dB at 1.035 b/sample.

### C. Noise Immunity

In order to assess the effectiveness of the proposed stopping criterion, we studied its performance to represent signals with different levels of added noise. This enables assessment of the capability of the method for discriminating signal from noise. To do this, we use the

$$\text{SNR} = 10\log_{10}\left(\frac{\| \mathbf{x} \|^2}{\| \mathbf{x} - \hat{\mathbf{x}}_q \|^2}\right)\text{dB} \tag{14}$$

where $\mathbf{x}$ is the original signal, and $\hat{\mathbf{x}}_q$ is the reconstructed signal using $q$ structures identified by the modeling algorithm.

Gaussian, i.i.d, noise signals of zero mean and energy of 0.0238 and 0.3237 were added to signal *S2*. The decompositions of those noisy signals have found six and three structures with SNRs of 36.57 and 19.73, respectively. The signals corresponding to the noisiest case can be observed in Fig. 9 (for the less noisy, there is no visually perceivable difference). The algorithm identifies successfully and precisely the structures whose energy is larger than the noise energy. We see that a small energy noise does not influence the choice of the atoms used to represent the signal; however, they influence the number of structures used (this is based on the mean approximation ratio, i.e., more added noise leads to earlier occurrence of noise-like representation). Therefore, the addition of a small amount of noise may help in obtaining faster decompositions, that is, the more noise added, the fewer terms (steps) the algorithm executes, and therefore, the smaller the overall computational complexity of the decomposition. As we can see, the algorithm is capable of sensing the presence of noise in the signal. This can be used to perform signal denoising by synthesis [4]. For example, if power system signals are corrupted by noise during the sampling process, such noise can be filtered by reconstructing the signal from the adaptive decomposition, as can be seen in Fig. 9.

## VII. Compression of Natural Signals

The decomposition algorithm was applied to measured signals from real power systems. As mentioned, this decomposition is meant to represent the signals by obtaining their coherent structures, yielding good compression ratios with low distortion. Oscillographic signals are often post-analyzed by experts (human or system) in order to gain knowledge about the fault event. Thus, the compression must allow an accurate signal analysis, that is, the analysis made on the reconstructed signal must give the same results as the ones held on the original measured signal. This refers to the consistency concept discussed in Section II. We present below a simple method to quantize and encode the parameters of the structures. This procedure is such that high SNR, high compression, and accurate analysis are possible. Results confirming these conjectures are presented for natural signals.

### A. Quantization of Structures

The damped sinusoid structure obtained by the decomposition proposed, at each step $n$, is characterized by the six-tuple $\gamma(n) = [A(n), \rho(n), \xi(n), \phi(n), t_s(n), t_e(n)]$. We present a simple scheme to quantize this six-tuple. The starting and ending times (or samples) of the structures are quantized by a scalar quantizer of $\log_2 N$ bits, where $N$ is the signal length. The inner product at a given step $n$ of the decomposition $A(n)$, the damping factor $\rho(n)$, and the phase $\phi(n)$, can also be quantized by simple and independent fixed-rate scalar quantizers [32]. These quantizers are designed according to the dynamic range (minimum and maximum values) of each parameter for all the structures found in the signal. This is done by setting up a number of bits for each of these parameters. We refer to the number of bits used to quantize the inner product of the structures as $b_A$, the number of bits for the damping factor as $b_\rho$, and the number of bits for the phase as $b_\phi$. For frequency $\xi(n)$, a quantization that considers the sampling frequency $F_s$ and the fundamental frequency is used, as shown in Section V-B. In addition, a signal header is used to inform the models of the quantizers above, the signal length, the sampling frequency $F_s$, and the fundamental frequency $F$. In the experiments presented next, the header was 150 bits long.

One should note that after the decomposition finishes, the parameters are quantized with no update of the residues. Thus, this can be regarded as an off-line quantization, which in essence allows for a simple rate control scheme if desired. The quantization/encoding procedure presented a satisfactory performance to enable the assessment of the compression capability of the proposed decomposition.

### B. Results

Measured signals collected from fault events in the Brazilian power system were decomposed using the procedure presented. Those signals are shown in Fig. 10(a) (neutral current during a real fault—*R1*) and Fig. 11(a) (voltage phase during a real

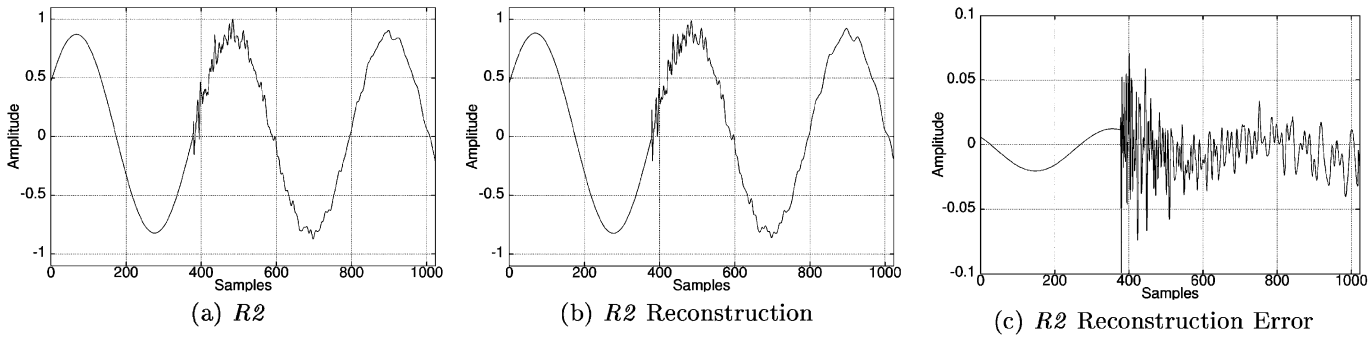


Fig. 11. Quantization of signal R2 with $b_A = 6$, $b_\rho = 6$, and $b_\phi = 6$, where the compression ratio is 27.40, and the SNR is 31.12 dB at 0.584 b/sample.

TABLE IV
TEN STRUCTURES OBTAINED AFTER DECOMPOSING SIGNAL *R2* AND QUANTIZING THE STRUCTURES WITH $b_A = 6$, $b_\rho = 6$, AND $b_\phi = 6$ (SEE FIG. 11)

| Structure | Amplitude | Frequency (in Hz) | $\rho$ | Phase (in Degrees) | $t_s$ (in samples) | $t_e$ (in samples) |
|---|---|---|---|---|---|---|
| 1 | 19.489243 | 60 | 0.000000 | 303.383514 | 0 | 1023 |
| 2 | 0.609039 | 0 | 0.000000 | 0.000000 | 0 | 1023 |
| 3 | 0.609039 | 2040 | 0.007807 | 113.768814 | 380 | 841 |
| 4 | 0.609039 | 600 | 0.000000 | 200.449829 | 397 | 1018 |
| 5 | 0.304519 | 3240 | 0.023422 | 92.098564 | 386 | 408 |
| 6 | 0.304519 | 2640 | 0.007807 | 281.713257 | 428 | 959 |
| 7 | 0.304519 | 900 | 0.000000 | 195.032257 | 395 | 973 |
| 8 | 0.304519 | 1680 | 0.003904 | 232.955185 | 378 | 919 |
| 9 | 0.304519 | 6960 | 0.238121 | 59.593189 | 379 | 382 |
| 10 | 0.304519 | 3900 | 0.000000 | 335.888855 | 389 | 472 |

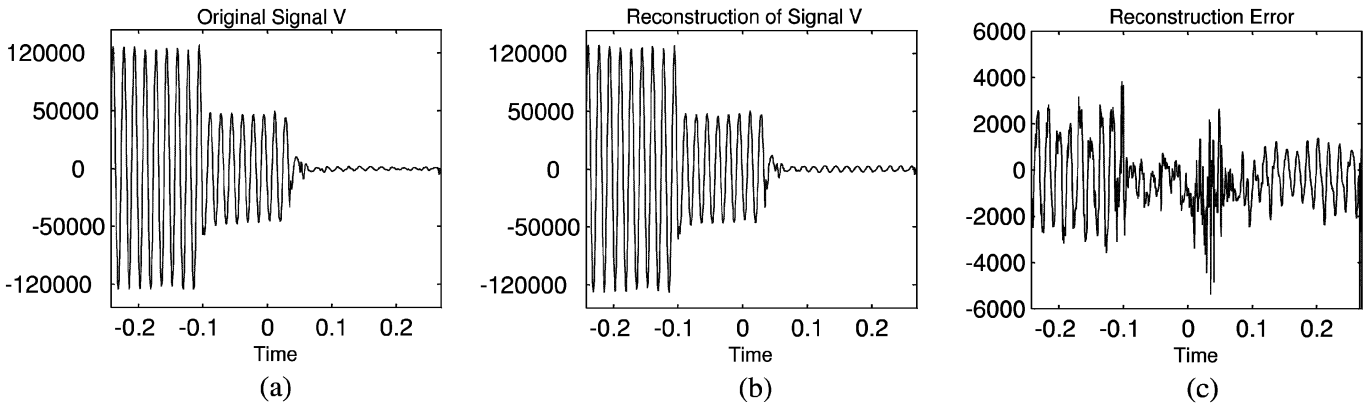


Fig. 12. Compression and reconstruction of the waveform of a fault. Compression Ratio $= 68.27$ and SNR $= 26.12$ dB.

fault—*R2*). *R1* was decomposed using 19 structures and *R2* using 20 structures prior to quantization. It is relevant to say that the first structure extracted from signal *R1* is $\gamma(1) = [7.451\,844,\ 0.004\,455,\ 956.947\,205,\ 11.489\,659,\ 432,\ 1023]$, where $t_s$ and $t_e$ are in samples, the fundamental frequency is 50 Hz, and the sampling frequency is 1000 Hz. After quantization, it becomes $\gamma(1) = [7.440\,485,\ 0.004\,839,\ 950,\ 10.683\,165,\ 432,\ 1023]$. Table IV presents the ten structures that represent signal *R2* after quantization. The compression ratio is defined as the overall bit rate of the original signal divided by the total number of bits used to represent the structures of the signal and the header. The original signals were stored in single-precision floating-point [using 16 bits per sample (b/sample)] and with no header, and the compression ratios were computed with respect to this format. The quality of the compressed signal *R1* can be verified visually in Fig. 10(b) and from its reconstruction error in Fig. 10(c). The same can be observed for signal *R2* in Fig. 11. Note that in these examples, the reconstruction error is computed after the quantization of the structures, and they can be diminished as we improve the quantization or reduce the compression ratio.

From these figures, we see that the results obtained are promising in that high compression ratios can be achieved along with high SNR. In addition, the important phenomena represented in the signal (according to the damped sinusoids model of Section III) are preserved. Since we use quantizers with a dead zone [33], the number of bits used to quantize the amplitude has a direct influence on the number of structures used to represent the signal after the quantization process. In addition, since $b_\rho$ and $b_\phi$ determine the quantization error of these parameters, the representations improve as they are increased. Therefore, they yield a compromise between compression ratio and reconstruction quality. We should also point out that the optimal selection of the number of bits used to

quantize each of the three parameters is not straightforward and deserves further study. In addition, vector quantization [32] and context coding schemes [33] could be investigated. For example, it is expected that frequency and damping factor have some correlation between them, and exploitation of such correlation may lead to further rate-distortion improvements.

In Fig. 12, we present another natural signal: a voltage $V$ from a transmission line where a fault has occurred. In Fig. 12(a), the original signal is presented, in Fig. 12(b), the compressed one (after quantization) is presented, and in Fig. 12(c), the reconstruction error is presented. To objectively assess the compression algorithm, when used in a signal analysis framework, we have analyzed both the original and compressed signals of Fig. 12 by filtering the fundamental frequency contribution [29]. The maximum percentile errors were 1.25% and 4.75% for modulus and angle, respectively, which is indeed a good result.

Note that the compression ratio is not a fair measure of the performance of the proposed method because if the sampling rates of the signal and of the dictionary change by the same amount, then the signal decomposition will undergo little change. In other words, the bit stream obtained would be the same (the only difference would be in the number of bits used to quantize the frequency, implying the addition of a small number of bits per structure). Thus, the compression ratio increases almost linearly as a function of the sampling rate of the signal.

## VIII. Conclusions

We proposed a compression algorithm for signals measured during power system disturbances that obtains good compression ratios while preserving important features for signal analysis. The algorithm decomposes a signal into a set of damped sinusoids through an adaptive algorithm (MP), that is, it represents the signal $\mathbf{x}$ as a sequence of inner products $\alpha_n = \langle \mathbf{R}_{\mathbf{x}}^{n-1}, \mathbf{g}_{\gamma(n)} \rangle$ and indexes $\gamma(n)$, where $n$ is the step. Each damped sinusoid $\mathbf{g}_{\gamma(n)}$ is represented by a set of parameters $\gamma = (f, \rho, \phi, t_s, t_e)$. We have developed procedures to accomplish the search in this five-parameter space in a computationally feasible and effective fashion.

The decomposition presented is coherent since it yields a representation that is related to the phenomena represented in the signal, that is, robust to noise, and that can be quantized effectively while maintaining the signal characteristics and preserving the proportions of the signal phenomena.

This work has also presented methods to obtain a representation of a signal based on damped sinusoids together with procedures to eliminate post-echo and pre-echo errors that often appear on greedy decomposition algorithms. We have also shown ways to correct the false phenomena identification that tends to occur when standard MP is used. In addition, there have been devised ways to decide how many atoms to use in order to decompose a signal based on the approximation ratio.

As suggestions for further research and improvements, we should mention that further studies in the discretization of the damped sinusoid's parameter space $(\gamma)$ is welcome. In addition, it is worthy to include into the model parameterized functions to represent inrush currents, as well as an approach using nonquantized frequency to model interharmonic frequency components. This would enable the elimination of sub-synchronous components that are components of frequency near the fundamental that are not multiples of it, which impair the analysis of oscillographic signal. In addition, the decomposition procedure that we present could be applied to other types of signals composed of damped sinusoids and suited to harmonic analysis, such as audio.

## References


[1] M. A. M. Rodrigues, M. V. F. de Figueiredo, A. L. L. Miranda, and S. S. Diniz, "Oscillography for power system operational planning," in *Proc. Symp. Specialists Electric Operational Expansion Planning*, Curitiba, Brazil, May 2000.

[2] S. Mallat and Z. Zhang, "Matching pursuits with time-frequency dictionaries," *IEEE Trans. Signal Process.*, vol. 41, no. 12, pp. 3397–3415, Dec. 1993.

[3] V. K. Goyal, M. Vetterli, and N. T. Thao, "Quantized overcomplete expansions in $\mathbb{R}^N$: Analysis, synthesis, and algorithms," *IEEE Trans. Inf. Theory*, vol. 44, no. 1, pp. 16–31, Jan. 1998.

[4] S. Mallat, *A Wavelet Tour of Signal Processing*. San Diego, CA: Academic, 1998.

[5] M. M. Goodwin and M. Vetterli, "Matching pursuits and atomic signal models based on recursive filters banks," *IEEE Trans. Signal Process.*, vol. 47, no. 7, pp. 1890–1902, Jul. 1999.

[6] G. Davis, "Adaptive Nonlinear Approximations," Ph.D. dissertation, Courant Inst. Mathematical Sci., New York Univ., New York, NY, 1994.

[7] D. L. Donoho, M. Vetterli, R. A. DeVore, and I. Daubechies, "Data compression and harmonic analysis," *IEEE Trans. Inf. Theory*, vol. 44, no. 5, pp. 2435–2476, Oct. 1998.

[8] O. K. Al-Shaykh, E. Miloslavsky, T. Nomura, R. Neff, and A. Zakhor, "Video compression using matching pursuits," *IEEE Trans. Circuits Syst. Video Technol.*, vol. 9, no. 2, pp. 123–143, Feb. 1997.

[9] H. Krim, D. Tucker, S. Mallat, and D. Donoho, "On denoising and best signal representations," *IEEE Trans. Inf. Theory*, vol. 45, no. 6, pp. 2225–2238, Nov. 1999.

[10] M. M. Goodwin, *Adaptive Signal Models: Theory, Algorithms, and Audio Applications*, First ed. New York: Kluwer, 1998.

[11] S. Chen and D. Donoho, "Basis pursuit," in *Proc. 28th Asilomar Conf. Signals, Syst., Comput.*, vol. 1, Sep. 1994, pp. 41–44.

[12] J. Adler, B. D. Rao, and K. Kreutz-Delgado, "Comparison of basis selection methods," in *Proc. 30th Asilomar Conf. Signals, Syst., Comput.*, vol. 1, Nov. 1996, pp. 252–257.

[13] G. Davis, S. Mallat, and Z. Zhang, "Adaptive Time-Frequency Approximations With Matching Pursuits," Courant Inst. Math. Sci., New York Univ., New York, NY, 1999.

[14] W. Xu, "Component modeling issues for power quality assessment," *IEEE Power Eng. Rev.*, vol. 21, no. 11, pp. 12–15, Nov. 2001.

[15] L. Lovisolo, E. A. B. da Silva, M. A. M. Rodrigues, and P. S. R. Diniz, "Coherent decompositions of power systems signals using damped sinusoids with applications to denoising," in *Proc. IEEE ISCAS*, vol. V, Scottsdale, AZ, May 2002, pp. 685–688.

[16] M. A. M. Rodrigues, "Efficient Decompositions for Signal Coding," Ph.D. dissertation, COPPE/UFRJ, Rio de Janeiro, RJ, Brazil, 1999.

[17] B. J. Bujanowski, J. W. Pierre, S. M. Hietpas, T. L. Sharpe, and D. A. Pierre, "A comparison of several system identification methods with application to power systems," in *Proc. 36th Midwest Symp. Circuits Syst.*, 1993.

[18] T. Lobos, J. Rezmer, and H.-J. Koglin, "Analysis of power systems transients using wavelets and Prony method," in *Proc. IEEE Porto Power Tech Conf.*, Porto, Portugal, 2001.

[19] M. M. Tawfik and M. M. Morcos, "ANN-based techniques for estimating fault location on transmission lines using Prony method," *IEEE Trans. Power Del.*, vol. 16, no. 2, pp. 219–224, Apr. 2001.

[20] I. Daubechies, *Ten Lectures on Wavelets*. Philadelphia, PA: Society for Industrial and Applied Mathematics, 1991.

[21] W. H. Press, S. A. Teukolsky, W. T. Vetterling, and B. P. Flannery, *Numerical Recipes in C—Theory of Scientific Computing*, Second ed. New York: Cambridge Univ Press, 1997.

[22] S. Jaggi, W. C. Carl, S. Mallat, and A. S. Willsky, "High resolution pursuit for feature extraction," *Appl. Comput. Harmon. Anal.*, vol. 5, no. 4, pp. 428–449, Oct. 1998.

[23] S. E. Ferrando, L. A. Kolasa, and N. Kovacevic, "Algorithm 820: A flexible implementation of matching pursuit for gabor functions on the interval," *ACM Trans. Math. Softw.*, vol. 28, pp. 337–353, Sep. 2002.

[24] A. W. Galli, G. T. Heydt, and P. F. Ribeiro, "Exploring the power of wavelet analysis," *IEEE Comput. Applicat. Power*, vol. 9, no. 4, pp. 37–41, Oct. 1996.
[25] J. Chung, E. J. Powers, W. M. Grady, and S. C. Bhatt, "Electric power transient disturbance classification using wavelet-based hidden Markov models," in *Proc. IEEE ICASSP*, 2000.
[26] R. A. DeVore and V. N. Temlyakov, "Some remarks in greedy algorithms," *Adv. Comput. Math.*, vol. 5, pp. 173–187, 1996.
[27] R. Heusdens, R. Vafin, and W. B. Kleijn, "Sinusoidal modeling using psychoacoustic-adaptive matching pursuits," *IEEE Signal Process. Lett.*, vol. 9, no. 8, pp. 262–265, Aug. 2002.
[28] R. Heusdens and S. van de Par, "Rate-distortion optimal sinusoidal modeling of audio and speech using psychoacoustical matching pursuits," in *Proc. IEEE ICASSP*, vol. 2, Orlando, FL, May 2002, pp. 1809–1812.
[29] E. O. Schweitzer III and D. Hou, "Filtering for protective relays," in *Proc. 47th Annu. Georgia Tech Protective Relaying Conf.*, Atlanta, GA, Apr. 1993.
[30] *EMTP Rule Book, Alternative Transients Rule Book*: Canadian-American EMTP User Group, 1987–1992.
[31] Y. C. Pati, R. Rezaiifar, and P. S. Krishnaprasad, "Orthogonal matching pursuit: Recursive function approximation with applications to wavelet decompositions," in *Proc. 27th Annual Asilomar Conf. Signals, Syst., Comput.*, Nov. 1993.
[32] A. Gersho and R. M. Gray, *Vector Quantization and Signal Compression*. Boston, MA: Kluwer, 1992.
[33] K. Sayood, *Introduction to Data Compression*, Second ed. San Francisco, CA: Morgan Kauffman, 2000.

**Lisandro Lovisolo** received the engineering degree in electronics and the M.Sc. degree in electrical engineering from the Federal University of Rio de Janeiro (UFRJ), Rio de Janeiro, Brazil, in 1999 and 2001, respectively. He is now pursuing the D.Sc. degree at the Signal Processing Laboratory (LPS), UFRJ.

Since 2003, he has been with the Department of Electronics and Telecommunications Engineering, State University of Rio de Janeiro (UERJ). His research interests are in signal processing, especially adaptive and overcomplete signal/image decompositions for analysis and coding purposes.

**Eduardo A. B. da Silva** (M'96) was born in Rio de Janeiro, Brazil, in 1963. He received the Engineering degree in electronics from the Instituto Militar de Engenharia (IME), Rio de Janeiro, in 1984, the M.Sc. degree in electronics from Universidade Federal do Rio de Janeiro (COPPE/UFRJ) in 1990, and the Ph.D. degree in electronics from the University of Essex, Essex, U.K., in 1995.

In 1987 and 1988, he was with the Department of Electrical Engineering, IME. Since 1989, he has been with the Department of Electronics Engineering, UFRJ. He has also been with the Department of Electrical Engineering, COPPE/UFRJ, since 1996. He has been head of the Department of Electrical Engineering, COPPE/UFRJ, Brazil, since 2002. His research interests lie in the fields of digital signal and image processing, especially signal coding, wavelet transforms, mathematical morphology, and applications to telecommunications.

Dr. da Silva won the British Telecom Postgraduate Publication Prize in 1995 for his paper on aliasing cancellation in subband coding. He is also co-author of the book *Digital Signal Processing—System Analysis and Design* (Cambridge, U.K.: Cambridge University Press, 2002), which has been translated into Chinese and Portuguese. He was a Distinguished Lecturer of the IEEE Circuits and Systems Society in 2003 and 2004.

**Marco A. M. Rodrigues** (M'88) was born in Rio de Janeiro, Brazil, in 1964. He received the engineering degree in electronics and the M.Sc. and the D.Sc. degrees in electrical engineering from the University of Rio de Janeiro in 1986, 1991, and 1999, respectively.

He has been with the Electric Power Research Center (CEPEL), Rio de Janeiro, since 1987, in data acquisition systems design, software design, algorithms for data analysis and control, and signal processing applications related to power systems. He is also an invited professor of a post-graduate course in protection for power systems, University of Rio de Janeiro. His current research interests are signal processing, power system measurements, oscillographic analysis automation, and power system protection systems.

Dr. Rodrigues is a member of Conseil International des Grands Réseaux Électriques (Cigré) and the Brazilian Telecommunications Society (SBrT) and was on the steering committee of the Brazilian Protection and Control Technical Seminary (STPC) in 2003 and 2005.

**Paulo S. R. Diniz** (F'00) was born in Niteroi, Brazil. He received the Electronics Eng. degree (cum laude) from the Federal University of Rio de Janeiro (UFRJ), Rio de Janeiro, Brazil, in 1978, the M.Sc. degree from COPPE/UFRJ in 1981, and the Ph.D. from Concordia University, Montreal, PQ, Canada, in 1984, all in electrical engineering.

Since 1979, he has been with the undergraduate Department of Electronic Engineering, UFRJ. He has also been with the graduate Program of Electrical Engineering, COPPE/UFRJ, since 1984, where he is presently a Professor. He served as Undergraduate Course Coordinator and as Chairman of the Graduate Department. He is one of the three senior researchers and coordinators of the National Excellence Center in Signal Processing

From January 1991 to July 1992, he was a visiting Research Associate with the Department of Electrical and Computer Engineering, University of Victoria, Victoria, BC, Canada. He also holds a Docent position at Helsinki University of Technology, Helsinki, Finland. From January 2002 to June 2002, he was a Melchor Chair Professor with the Department of Electrical Engineering, University of Notre Dame, Notre Dame, IN. His teaching and research interests are in analog and digital signal processing, adaptive signal processing, digital communications, wireless communications, multirate systems, stochastic processes, and electronic circuits. He has published several refereed papers in some of these areas and wrote the books *Adaptive Filtering: Algorithms and Practical Implementation* (Boston, MA; Kluwer, 2002, second ed.), and *Digital Signal Processing: System Analysis and Design* (Cambridge, U.K.: Cambridge Univ. Press, 2002) (with E. A. B. da Silva and S. L. Netto)

Dr. Diniz received the Rio de Janeiro State Scientist award from the Governor of Rio de Janeiro state. He was the Technical Program Chair of the 1995 MWSCAS held in Rio de Janeiro, Brazil. He has been on the technical committee of several international conferences including ISCAS, ICECS, EUSIPCO, and MWSCAS. He has served Vice President for region 9 of the IEEE Circuits and Systems Society and as Chairman of the DSP technical committee of the same society. He was elected Fellow of IEEE for fundamental contributions to the design and implementation of fixed and adaptive filters and electrical engineering education. He served as associate editor for the IEEE TRANSACTIONS ON CIRCUITS AND SYSTEMS II: ANALOG AND DIGITAL SIGNAL PROCESSING from 1996 to 1999, the IEEE TRANSACTIONS ON SIGNAL PROCESSING from 1999 to 2002, and the *Circuits, Systems and Signal Processing* from 1998 to 2002. He was a distinguished lecturer of the IEEE Circuits and Systems Society from 2000 to 2001. In 2004, he is serving as Distinguished Lecturer of the IEEE Signal Processing Society.